Implementing and Accelerating HMMER3 Protein Sequence Search on CUDA-Enabled GPU

Lin Cheng

A thesis

in

The Department

of

Computer Science and Software Engineering

Presented in Partial Fulfilment of the Requirements
For the Degree of Master of Computer Science
Concordia University
Montréal, Québec, Canada

July 2014

CONCORDIA UNIVERSITY

School of Graduate Studies

This is to certify that the thesis prepared

By :   **Lin Cheng**

Entitled :   **Implementing and Accelerating HMMER3 Protein Sequence Search on CUDA-Enabled GPU**

and submitted in partial fulfilment of the requirements for the degree of

Master of Computer Science

complies with the regulations of this University and meets the accepted standards with respect to originality and quality.

Signed by the final examining committee :

_____ Chair
Dr. A.

_____ Examiner
Dr. B.

_____ Examiner
Dr. C.

_____ Supervisor
 Dr. Gregory Butler

Approved by   _____
Dr. D.
Chair of Department or Graduate Program Director

_____   2014.   _____
Dr. E.
Dean of Faculty
(Computer Science and Software Engineering)

CONCORDIA UNIVERSITY

Computer Science and Software Engineering

Abstract

Implementing and Accelerating HMMER3 Protein Sequence Search on CUDA-Enabled GPU

by Lin CHENG

The recent emergence of multicore CPU and manycore GPU architectures has made parallel computing more accessible. Hundreds of industrial and research applications have been mapped onto GPUs to further utilize the extra computing resource. In bioinformatics, HMMER is a set of widely used applications for sequence analysis based on Hidden Markov Model. One of the tools in HMMER, *hmmsearch*, and the Smith-Waterman algorithm are two important tools for protein sequence analysis that use dynamic programming. Both tools are particularly well-suited for many-core GPU architecture due to the parallel nature of sequence database searches.

After studying the existing research on CUDA acceleration in bioinformatics, this thesis investigated the acceleration of the key Multiple Segment Viterbi algorithm in HMMER version 3. A fully-featured CUDA-enabled protein database search tool *cudaHmmsearch* was designed, implemented and optimized. We demonstrated a variety of optimization strategies that are useful for general purpose GPU-based applications. Based on our optimization experience in parallel computing, six steps were summarized for optimizing performance using CUDA programming.

We made comprehensive tests and analysis for multiple enhancements in our GPU kernels in order to demonstrate the effectiveness of selected approaches. The performance analysis showed that GPUs are able to deal with intensive computations, but are very sensitive to random accesses to the global memory. The results show that our implementation achieved 2.5x speedup over the single-threaded HMMER3 CPU SSE2 implementation on average.

Acknowledgements

Contents

List of Figures

List of Tables

Abbreviations

CUDA	**C**ompute **U**nified **D**evice **A**rchitecture
DMA	**D**irect **M**emory **A**ccess
DP	**D**ynamic **P**rogramming
GPU	**G**raphics **P**rocessing **U**nit
HMM	**H**idden **M**arkov **M**odel
HMMER	**H**idden **M**arkov **M**odel**ER**
MPI	**M**essage **P**assing **I**nterface
MSV	**M**ultiple **S**egment **V**iterbi
NCBI	**N**ational **C**enter for **B**iotechnology **I**nformation)
NR	**N**on-**R**edundant
OS	**O**perating **S**ystem
Pfam	**P**rotein **fam**ilies
SIMD	**S**ingle-**I**nstruction **M**ultiple-**D**ata
SM	**S**treaming **M**ultiprocessors
SSE	**S**treaming **SIMD** **E**xtensions
SW	**S**mith-**W**aterman

Chapter 1

Introduction

1.1   Problem Statement

A protein can be viewed as a sequence of amino acid residues. In Bioinformatics, the purpose of protein sequence search against databases is to identify regions of similarity that may be a consequence of functional, structural, or evolutionary relationships between the protein sequences. Such a similarity search produces an alignment, i.e. seeks to align similar substrings of the sequences being compared.

Classical sequence alignment algorithms such as Needleman-Wunsch [Needleman and Wunsch, 1970], Smith-Waterman [Smith and Waterman, 1981], and the BLAST family of programs [Altschul et al., 1990] have long been used for searching protein by performing pairwise alignment of each query against every sequence in the database, thus identifying those sequences in the database that are most closely related to various regions of the query.

Besides the above pairwise comparison algorithms, another paradigm compares a sequence to a probabilistic representation of several proteins of the same family. Since all the sequences in a family are mostly similar to each other, it is possible to construct a common profile representing the *consensus sequence*, which simply reflects the most commonly occurring residue at each position. One such probabilistic representation is called the *profile HMM* (Hidden Markov Model) introduced by Anders Krogh and David Haussler [Krogh et al., 1994], which is a promising approach to improve the sensitivity of database-searching.

The profile HMM is a statistical model of a multiple sequence alignment, or even of a single sequence. The main strength of a profile HMM is that it is probabilistic finite state machine. This means that it assesses the probability of match, insert and delete at a given position of an alignment.

Unlike conventional pairwise comparisons, a consensus profile HMM model can in principle utilize additional statistical information, such as the position and identity of residues that are more or less conserved throughout the family, as well as variable insertion and deletion probabilities. By developing a statistical model that is based on known sequences in a protein family, a profile HMM can be used to model the protein sequence family.

In Bioinformatics, HMMER [HMMER, 2014b] is a free and commonly used software package for sequence analysis based on the profile HMM. Based on the strength of its underlying profile HMMs, HMMER aims to be significantly more accurate and more able to detect remote homologs, compared to BLAST, FASTA, and other sequence alignment tools and database search tools [Eddy, 2011].

From 1992 to 1998, the HMMER1 series was developed by Sean Eddy. It includes a feature that is missing in HMMER2 and HMMER3: the *hmmt* program for training HMMs from initially unaligned sequences and hence creating multiple alignments. The final stable version of HMMER1 was released as 1.8.5 in 2006.

From 1998 to 2003, the HMMER2 series introduced the "Plan 7" profile HMM architecture, which is still shared with HMMER3, and was the basic foundation for Pfam and other protein domain databases. It includes local and global alignment modes that HMMER3 lacks, because HMMER3 currently implements only fully local alignment. HMMER2 lacks DNA comparison that was present in HMMER1. The final stable version of HMMER2 was released as 2.3.2 in 2003.

In HMMER, the application *hmmbuild* is used to build a profile HMM using a multiple sequence alignment, or single sequence as input. The application *hmmsearch* is used to search a profile HMM against a sequence database, finding whether a sequence is member of the family described by the profile HMM. The *hmmsearch* application outputs a ranked list of the sequences with the most significant matches to the profile. Another

similar application in HMMER, *hmmscan*, is the query of a single protein sequence of interest against a database of profile HMMs.

To compare a profile HMM with a protein sequence, HMMER uses the Viterbi algorithm detailed in subsection 2.2.2.2, which evaluates the path that has the maximum probability of the profile HMM generating the sequence. The Viterbi algorithm is a dynamic programming algorithm. The fundamental task of the Viterbi algorithm for biological sequence alignment is to calculate three DP (Dynamic Programming) matrices: $M[\ ]$ for Match state, $I[\ ]$ for Insert state and $D[\ ]$ for Delete state. Each element value in the DP matrix is dependent on the value of previous element.

However, the widely used implementation of the Viterbi algorithm in HMMER2, has been slow and compute-intensive, on the order of more than 100 times slower than BLAST for a comparable search. In an era of enormous sequence databases, this speed disadvantage outweighs any advantage of the profile HMM method.

With the exponential growth of protein databases, there is an increasing demand for acceleration of such techniques. HMMER has been a target of many acceleration and optimization efforts.

Specialized hardware architectures have been used to exploit coarse-grained parallelism in accelerating HMMER2. JackHMMer [Wun et al., 2005] uses the Intel IXP 2850 network processor. [Maddimsetty, 2006], [Derrien and Quinton, 2007] and [Oliver et al., 2007] use FPGAs (Field-Programmable Gate Arrays). Sachdeva et al. use the Cell Broadband Engine developed by IBM [Sachdeva et al., 2008].

On traditional CPU architecture, MPI-HMMER [Walters et al., 2006] is a well-known and commonly used MPI implementation. In their studies, a single master node is used to assign multiple database blocks to worker nodes for computing in parallel and is responsible for collecting the results. Landman et al. exploit MPI and Intel SSE2 intrinsics to accelerate HMMER2 [Landman et al., 2006].

Graphics Processing Unit (GPU), as a specialized processor originally intended for manipulating computer graphics, has been shown to provide very attractive compute resources in addition to CPU and the above specialized hardware architectures, because of particular manycore parallel computation in a modern GPU.

Based on the GPUs produced by NVIDIA, NVIDIA introduced CUDA (Computer Unified Device Architecture) to facilitate general-purpose computing on GPUs. NVIDIA also developed the CUDA C/C++ compiler, libraries, and runtime software to enable programmers to access the GPU parallel computing capabilities.

ClawHMMer [Horn et al., 2005] is the first GPU-enabled *hmmsearch* implementation. Their implementation is based on the BrookGPU stream programming language, not the CUDA programming model. Since ClawHMMer, there has been several researches on accelerating HMMER for CUDA-enabled GPU. [Walters et al., 2009], [Ganesan et al., 2010], [Du et al., 2010] and [Quirem et al., 2011] parallelized the Viterbi algorithm on CUDA-enabled GPUs. However, these efforts have had limited impact on accelerating HMMER2 with speedups of only an order of magnitude.

In 2010, HMMER3.0 was released. It is the most significant acceleration of hmmsearch. The most significant difference between HMMER3 and HMMER2 is that HMMER3 uses a heuristic algorithm called the MSV filter, for Multiple (local, ungapped) Segment Viterbi, to accelerate profile HMM searches. By using the Intel SSE2 intrinsics to implement programs, HMMER3 is substantially more sensitive, and 100 to 1000 times faster than HMMER2 [Eddy, 2011].

HMMER3.1 beta was released in 2013. It has several new features that did not make them into 3.0, including *nhmmer* program for DNA homology searches with profile HMMs, the parallel search daemon *hmmpgmd* program underlying HMMER Web Services, and a new HMM file format called 3/f format.

Although HMMER3 is much faster than HMMER2 and about as fast as BLAST for protein searches, it is still time-consuming. According to the CPU Benchmarks [PassMark, 2014] updated on 17th of June 2014, the Intel Core i7-3930K @ 3.20GHz ranks as the 2nd among 'Common CPUs' and as the 23rd among 'High End CPUs' in terms of performance. Our benchmark result in Section 4.2.2 shows that even run by this high power CPU, HMMER3 needs about 5 minutes to search a profile HMM with length 255 against the NCBI NR database.

[Ahmed et al., 2012] uses Intel VTune Analyzer [Intel, 2013] to investigate performance hotspot functions in HMMER3. Based on hotspot analysis, they study CUDA acceleration for three individual algorithms: Forward, Backward and Viterbi.

According to the implementation of HMMER3 detailed in Figure 3.1, the MSV, Viterbi, Forward and Backward algorithms are implemented in the so-called "acceleration pipeline" at the core of the HMMER3 software package [Eddy, 2011]. The MSV algorithm is the first filter of the "acceleration pipeline" and is the key hotspot of the whole process. Therefore, this thesis concentrates on porting the MSV filter onto a CUDA-enabled GPU to accelerate the *hmmsearch* application.

1.2   Research Objectives

The objective of this research is to *implement and accelerate hmmsearch of HMMER3 on a CUDA-enabled GPU*. Our implementation will be based on the HMMER3 MSV algorithm so that the result will be same as the *hmmsearch* of HMMER3. Central to this goal is understanding the MSV algorithm and CUDA multi-thread parallel programming.

In Bioinformatics, Smith-Waterman algorithm is also famous for sequence alignment using dynamic programming. Instead of looking at the total sequence, the Smith-Waterman algorithm compares segments of all possible lengths and optimizes the similarity measure. Similar to the MSV algorithm, the Smith-Waterman algorithm is also fairly demanding of time: to align two sequences of lengths m and n, $O(\mathrm{mn})$ time is required. There has been a great deal of research on accelerating the Smith-Waterman algorithm on a CUDA-enabled GPU. From studying these research, we learn many optimization approaches to apply into our research.

1.3   Research Contributions

The contribution of this thesis can be classified as follows:

- Analyze the core application *hmmsearch* in HMMER3 and find the key hotspot, the MSV filter, for accelerating hmmsearch.

- Implement the protein sequence search tool *cudaHmmsearch* on a CUDA-enabled GPU. Demonstrate many optimization approaches to accelerate cudaHmmsearch.

- Discuss and analyze the advantages and limitations of GPU hardware for CUDA parallel programming.

- Summarize the six steps for optimizing performance using CUDA programming.

1.4   Organization of thesis

The rest of this thesis is organized as follows:

Chapter 2 introduces the background necessary for understanding the work in this thesis.

Chapter 3 presents the details of our *cudaHmmsearch* implementation and optimization approaches. The six steps are summarized for better performance of CUDA programming at the end of this Chapter.

We performed comprehensive benchmarks which are presented and analyzed in Chapter 4.

The conclusion of Chapter 5 summarizes our contributions, points out its limitations, and makes suggestions for future work.

1.5   Typographical Conventions

The following font conventions are used in this thesis:

- Adobe Helvetica font
  Used for code examples.

- *Adobe Helvetica slanted font*
  Used for comments of code.

- Adobe AvantGarde font
  Used for captions of table, figure and listing.

Chapter 2

Background

The background of this thesis is concerned with the algorithms related to our work and how they were accelerated by many studies on CUDA-enabled GPUs. The first section briefly introduces the basic concepts about sequence alignment and protein database. The second section shows how the Smith-Waterman algorithms and the HMM-based algorithms use dynamic programming for sequence alignment and database searches. The third section overviews CUDA programming model and reviews recent studies on accelerating the Smith-waterman algorithm and the HMM-based algorithms on CUDA-enabled GPU.

2.1 Sequence alignment and protein database

2.1.1 Cells, amino acids and proteins

In 1665, Robert Hooke discovered the cell [Wiki Cell, 2014]. The cell theory, first developed in 1839 by Matthias Jakob Schleiden and Theodor Schwann, generalized the view that *all living organisms are composed of cells and of cell products* [Loewy et al., 1991]. As workhorses of the cell, proteins not only constitute the major component in the cell, but they also regulate almost all activities that occurs in living cells.

Proteins are complex chains of small organic molecules known as *amino acids*. In this thesis, *residue* is used to refer to the amino acids of a protein. The 20 amino acids detailed in Table 2.1 have been found within proteins and they convey a vast array of

chemical versatility. Hence proteins can be viewed as sequences of an alphabet of the 20 amino acids {A,C,D,E,F,G,H,I,K,L,M,N,P,Q,R,S,T,V,W,Y}.

Letter	Amino acid	Letter	Amino acid
A	Alanine	C	Cysteine
D	Aspartic acid	E	Glutamic acid
F	Phenylalanine	G	Glycine
H	Histidine	I	Isoleucine
K	Lysine	L	Leucine
M	Methionine	N	Asparagine
P	Proline	Q	Glutamine
R	Arginine	S	Serine
T	Threonine	V	Valine
W	Tryptophan	Y	Tyrosine

TABLE 2.1: The 20 amino acids

The following is the protein sequence of human beta globin taken from Swiss-Prot database. The sequence has a entry name HBB_HUMAN in Swiss-Prot database. The number beside the residue indicates the position of the residue.

```
HBB_HUMAN    1 MVHLTPEEKS AVTALWGKVN VDEVGGEALG RLLVVYPWTQ RFFESFGDLS 50
HBB_HUMAN   51 TPDAVMGNPK VKAHGKKVLG AFSDGLAHLD NLKGTFATLS ELHCDKLHVD 100
HBB_HUMAN  101 PENFRLLGNV LVCVLAHHFG KEFTPPVQAA YQKVVAGVAN ALAHKYH 147
```

LISTING 2.1: HBB_HUMAN protein sequence taken from Swiss-Prot

2.1.2 Sequence alignment

In bioinformatics, a sequence alignment of proteins is a way of arranging the sequences of the proteins to identify regions of similarity [Wiki Sequence, 2014]. If two amino acid sequences are recognized as similar, there is a chance that they are *homologous*. Homologous sequences share a common functional, structural, or evolutionary relationship. Protein sequences evolve by accumulating mutations. The basic mutational processes are *substitution*, where one residue is replaced by another, *insertion*, where a new residue is inserted into the sequence, and *deletion*, the removal of a residue. Insertion and deletion are together referred to as *gap* [Pevsner, 2009].

In the pairwise alignment shown in Listing 2.2, the sequence globins4 is on top and the sequence HBB_HUMAN is below. Note that this particular alignment is called *local* because only a subset of the two proteins is aligned: the first residue of HBB_HUMAN is not displayed. A global pairwise alignment includes all residues of both sequences. An intermediate row indicates the presence of *identical* residues in the alignment. Some of the aligned residues are similar but not identical (as indicated by the plus sign +); they are related to each other because they share similar biochemical properties. *Similar* pairs of residues are structurally or functionally related. For example, on the first part of the alignment we can find V and H connected by a + sign; nearby we can see S and T aligned in the same way. These are *conservative substitutions*. At the position 20 of HBB_HUMAN, an internal gap open and gap extend is indicated by two dashes.

```
  globins4    1 VVLSEAEKTKVKAVWAKVEADVEESGADILVRLFKSTPATQEFFEKFKDL 50
                V+L+++EK++V+A+W+KV  +V+E+G+++L RL++++P+TQ+FFE+F+DL
 HBB_HUMAN    2 VHLTPEEKSAVTALWGKV--NVDEVGGEALGRLLVVYPWTQRFFESFGDL 49


  globins4   51 STEDELKKSADVKKHGKKVLDALSDALAKLDEKLEAKLKDLSELHAKKLK 100
                ST+D+++++++VK+HGKKVL+A+SD+LA+LD +L++++++LSELH++KL+
 HBB_HUMAN   50 STPDAVMGNPKVKAHGKKVLGAFSDGLAHLD-NLKGTFATLSELHCDKLH 98


  globins4  101 VDPKYFKLLSEVLVDVLAARLPKEFTADVQAALEKLLALVAKLLASKYK 149
                VDP++F+LL++VLV+VLA++++KEFT++VQAA++K++A VA++LA+KY+
 HBB_HUMAN   99 VDPENFRLLGNVLVCVLAHHFGKEFTPPVQAAYQKVVAGVANALAHKYH 147
```

LISTING 2.2: Pairwise alignment of globins4 and HBB_HUMAN

```
 globins4    15 W A K V E A D V E E S G A D I L V R 32
                W + K V     + V + E + G + + + L   R
 HBB_HUMAN   16 W G K V - - N V D E V G G E A L G R 31
                ...............................................
 match          11  5 4       4   5   6       4   5
 mismatch        0           1   2   -2  0 2 -1  -3
 gap open               -11
 gap extend                -1
 sum of match: 11+5+4+4+5+6+4+5 = 44
 sum of mismatch: 0+1+2-2+0+2-1-3 = -1
 sum of gap penalties: -11-1 = -12
 total raw score: match + mismatch + gap penalties = 44-1-12 = 31
```

LISTING 2.3: Calculation of raw score.

To establish the degree of similarity, the two sequences are aligned: lined up in such a way that the similarity score is maximized. Listing 2.3 illustrates how raw scores are

calculated, using the result of pairwise alignment with just residues 15-32 of globins4 in Listing 2.2.

The scores in the Listing 2.3 for *match/mismatch* are taken from the scoring matrix BLOSUM62 as shown in Figure 2.1. The BLOSUM62 matrix is a substitution matrix used for sequence alignment of proteins. It were first introduced in a paper by S. Henikoff and J.G. Henikoff [Henikoff and Henikoff, 1992]. For example, the match score for W-W is 11, K-K is 5; the mismatch score for A-G is 0, D-N is 1.

In a typical scoring scheme there are two gap penalties: one for *gap open* (-11 for the position 19 of globins4 in Listing 2.3) and one for *gap extend* (-1 for the position 20 of globins4 in Listing 2.3).

```
     A   R   N   D   C   Q   E   G   H   I   L   K   M   F   P   S   T   W   Y   V   B   Z   X
A    4  -1  -2  -2   0  -1  -1   0  -2  -1  -1  -1  -1  -2  -1   1   0  -3  -2   0  -2  -1   0
R   -1   5   0  -2  -3   1   0  -2   0  -3  -2   2  -1  -3  -2  -1  -1  -3  -2  -3  -1   0  -1
N   -2   0   6   1  -3   0   0   0   1  -3  -3   0  -2  -3  -2   1   0  -4  -2  -3   3   0  -1
D   -2  -2   1   6  -3   0   2  -1  -1  -3  -4  -1  -3  -3  -1   0  -1  -4  -3  -3   4   1  -1
C    0  -3  -3  -3   9  -3  -4  -3  -3  -1  -1  -3  -1  -2  -3  -1  -1  -2  -2  -1  -3  -3  -2
Q   -1   1   0   0  -3   5   2  -2   0  -3  -2   1   0  -3  -1   0  -1  -2  -1  -2   0   3  -1
E   -1   0   0   2  -4   2   5  -2   0  -3  -3   1  -2  -3  -1   0  -1  -3  -2  -2   1   4  -1
G    0  -2   0  -1  -3  -2  -2   6  -2  -4  -4  -2  -3  -3  -2   0  -2  -2  -3  -3  -1  -2  -1
H   -2   0   1  -1  -3   0   0  -2   8  -3  -3  -1  -2  -1  -2  -1  -2  -2   2  -3   0   0  -1
I   -1  -3  -3  -3  -1  -3  -3  -4  -3   4   2  -3   1   0  -3  -2  -1  -3  -1   3  -3  -3  -1
L   -1  -2  -3  -4  -1  -2  -3  -4  -3   2   4  -2   2   0  -3  -2  -1  -2  -1   1  -4  -3  -1
K   -1   2   0  -1  -3   1   1  -2  -1  -3  -2   5  -1  -3  -1   0  -1  -3  -2  -2   0   1  -1
M   -1  -1  -2  -3  -1   0  -2  -3  -2   1   2  -1   5   0  -2  -1  -1  -1  -1   1  -3  -1  -1
F   -2  -3  -3  -3  -2  -3  -3  -3  -1   0   0  -3   0   6  -4  -2  -2   1   3  -1  -3  -3  -1
P   -1  -2  -2  -1  -3  -1  -1  -2  -2  -3  -3  -1  -2  -4   7  -1  -1  -4  -3  -2  -2  -1  -2
S    1  -1   1   0  -1   0   0  -1  -1  -2  -2   0  -1  -2  -1   4   1  -3  -2  -2   0   0   0
T    0  -1   0  -1  -1  -1  -1  -2  -2  -1  -1  -1  -1  -2  -1   1   5  -2  -2   0  -1  -1   0
W   -3  -3  -4  -4  -2  -2  -3  -2  -2  -3  -2  -3  -1   1  -4  -3  -2  11   2  -3  -4  -3  -2
Y   -2  -2  -2  -3  -2  -1  -2  -3   2  -1  -1  -2  -1   3  -3  -2  -2   2   7  -1  -3  -2  -1
V    0  -3  -3  -3  -1  -2  -2  -3  -3   3   1  -2   1  -1  -2   0  -3  -1   4  -3  -2  -1
B   -2  -1   3   4  -3   0   1  -1   0  -3  -4   0  -3  -3  -2   0  -1  -4  -3  -3   4   1  -1
Z   -1   0   0   1  -3   3   4  -2   0  -3  -3   1  -1  -3  -1   0  -1  -3  -2  -2   1   4  -1
X    0  -1  -1  -1  -2  -1  -1  -1  -1  -1  -1  -1  -1  -2   0   0  -2  -1  -1  -1  -1  -1
```

FIGURE 2.1: BLOSUM62 Scoring Matrix from http://www.ncbi.nlm.nih.gov/Class/FieldGuide/BLOSUM62.txt.

The next chapter will introduce two sequence alignment algorithms: the Smith-Waterman algorithm and two HMM-based algorithms. These algorithms share a very general optimization technique called dynamic programming for finding optimal alignments.

2.1.3 Bioinformatics protein databases

This part is a brief introduction of two protein sequence databases used in this thesis.

NCBI NR databse

The NCBI (National Center for Biotechnology Information) houses a series of databases relevant to Bioinformatics. Major databases include GenBank for DNA sequences and PubMed, a bibliographic database for the biomedical literature. Other databases include the NCBI Epigenomics database. All these databases are updated daily and available online: http://www.ncbi.nlm.nih.gov/guide/all/#databases_.

The NR (Non-Redundant) protein database maintained by NCBI as a target for their BLAST search services is a composite of Swiss-Prot, Swiss-Prot updates, PIR (Protein Information Resource), and PDB (Protein Data Bank). Entries with absolutely identical sequences have been merged into NR database. The PIR produces the largest, most comprehensive, annotated protein sequence database in the public domain. The PDB is a repository for the three-dimensional structural data of large biological molecules, such as proteins and nucleic acids and is maintained by Brookhaven National Laboratory, USA.

Release 2014_04 of NCBI NR databse contains 38,442,706 sequence entries, comprising 13,679,143,700 amino acids, more than 24GB in file size [NCBI, 2014].

Swiss-Prot

The Universal Protein Resource (UniProt) is a comprehensive resource for protein sequence and annotation data and is mainly supported by the National Institutes of Health (NIH) [UniProt, 2014]. The UniProt databases are the UniProt Knowledgebase (UniProtKB), the UniProt Reference Clusters (UniRef), and the UniProt Archive (UniParc).

The UniProt Knowledgebase is updated every four weeks on average and consists of two sections:

1. UniProtKB/Swiss-Prot

   This section contains manually-annotated records with information extracted from literature and curator-evaluated computational analysis. It is also highly cross-referenced to other databases. Release 2014_05 of 14-May-2014 of UniProtKB/Swiss-Prot contains 545,388 sequence entries, comprising 193,948,795 amino acids abstracted from 228,536 references [UniProtSP, 2014-05].

2. UniProtKB/TrEMBL

   This section contains computationally analyzed records that await full manual annotation. Release 2014_05 of 14-May-2014 of UniProtKB/TrEMBL contains 56,010,222 sequence entries, comprising 17,785,675,050 amino acids [UniProtTr, 2014-05].

2.2 Dynamic programming in Bioinformatics

Dynamic Programming (DP) is an optimization technique that recursively breaks down a problem into smaller subproblems, such that the solution to the larger problem can be obtained by piecing together the solutions to the subproblems [Baldi and Brunak, 2001]. This section shows how the Smith-Waterman algorithms and the algorithms in HMMER use DP for sequence alignment and database searches.

2.2.1 The Smith-Waterman algorithm

The Smith-Waterman algorithm is designed to find the optimal local alignment between two sequences. It was proposed by Smith and Waterman [Smith and Waterman, 1981] and enhanced by Gotoh [Gotoh, 1982]. The alignment of two sequences is based on the dynamic programming approach by computing the similarity score which is given in the form of similarity score matrix H.

Given a query sequence Q with length L_q and a target sequence T with length L_t, let S be the substitution matrix and its element $S[i, j]$ be the similarity score for the combination of the ith residue in Q and the jth residue in T. Define G_e as the gap extension penalty, and G_o as the gap opening penalty. These similarity scores and G_e, G_o are pre-determined by the life sciences community. The similarity score matrix H for aligning Q and T is calculated as

$$E[i, j] = max \begin{cases} E[i, j-1] - G_e \\ H[i, j-1] - G_o \end{cases}$$

$$F[i,j] = max \begin{cases} F[i-1,j] - G_e \\ H[i-1,j] - G_o \end{cases}$$

$$H[i,j] = max \begin{cases} 0 \\ E[i,j] \\ F[i,j] \\ H[i-1,j-1] + S[i,j] \end{cases}$$

where $1 \leqslant i \leqslant L_q$ and $1 \leqslant j \leqslant L_t$. The values for E, F and H are initialized as $E[i,0] = F[0,j] = H[i,0] = H[0,j]$ when $0 \leqslant i \leqslant L_q$ and $0 \leqslant j \leqslant L_t$.

The maximum value of the matrix H gives the similarity score between Q and T.

2.2.2   HMMER

HMMER [HMMER, 2014b] is a set of applications that create a profile Hidden Markov Model (HMM) of a sequence family which can be utilized as a query against a sequence database to identify (and/or align) additional homologs of the sequence family[Markel and Leon, 2003]. HMMER was developed by Sean Eddy at Washington University and has become one of the most widely used software tools for sequence homology. The main elements of this HMM-based sequence alignment package are *hmmsearch* and *hmmscan*. The former searches a profile HMM against a sequence database, while the latter searches a sequence against a database of profile HMMs .

2.2.2.1   HMM and profile HMM

A hidden Markov model (HMM) is a computational structure for linearly analyzing sequences with a probabilistic method [Hancock and Zvelebil, 2004]. HMMs have been widely used in speech signal, handwriting and gesture detection problems. In bioinformatics they have been used for applications such as sequence alignment, prediction of protein structure, analysis of chromosomal copy number changes, and gene-finding algorithm [Pevsner, 2009].

A HMM is a type of a non-deterministic finite state machine with transiting to another state and emitting a symbol under a probabilistic model. According to [Dong and Pei, 2007], a HMM can be defined as a 6-tuple (A, Q, q_0, q_e, tr, e) where

- A is a finite set (the alphabet) of symbols;

- Q is a finite set of *states*;

- q_0 is the *start* state and q_e is the *end* state;

- tr is the *transition* mapping, which is the transition probabilities of state pairs in $Q \times Q$, satisfying the following two conditions:

  (a) $0 \leqslant tr(q, q') \leqslant 1$, $\forall q, q' \in Q$, and

  (b) for any given state q, such that:

$$\sum_{q' \in Q} tr(q, q') = 1$$

- e is the *emission* mapping, which is the emission probabilities of pairs in $Q \times A$, satisfying the following two conditions:

  (a) $0 \leqslant e(q, x) \leqslant 1$, if it is defined, $\forall q \in Q$, and $x \in A$

  (b) for any given state q,

   either (i) if for any $x \in A$, $e(q, x)$ is defined, then q is an *emitting* state and

$$\sum_{x \in A} e(q, x) = 1$$

   or (ii) if $\forall x \in A$, $e(q, x)$ is not defined, then q is a *silent* state.

The dynamics of the system are based on Markov Chain, meaning that only the current state influences the selection of its successor – the system has no 'memory' of its history. Only the succession of characters emitted is visible; the state sequence that generated the characters remains internal to the system, i.e. hidden. Hence, the name is Hidden Markov Model[Lesk, 2008].

A profile HMM is a variant of HMM and can be constructed from an initial multiple sequence alignment to define a set of probabilities. The symbol sequence of an HMM is

an observed sequence that resembles a consensus for the multiple sequence alignment. A protein family can be defined by a profile HMM.

In Figure 2.2, the internal structure of the "Plan 7" profile HMM used by HMMER[Eddy, 2011] shows the mechanism for generating sequences. In order to generate sequences, a profile HMM should have a set of three states per alignment column: one *match* state, one *insert* state and one *delete* state.

- **A match state** matches and emits a amino acid from the query. The probability of emitting each of the 20 amino acids is a property of the model.

- **An insert state** allows the insert of one or more amino acids. The emission probability of this state is computed either from a background distribution of amino acids or from the observed insertions in the alignment.

- **A delete state** skips the alignment column and emits a blank. Entering this state corresponds to gap opening, and the probabilities of these transitions reflect a position-specific gap penalty.
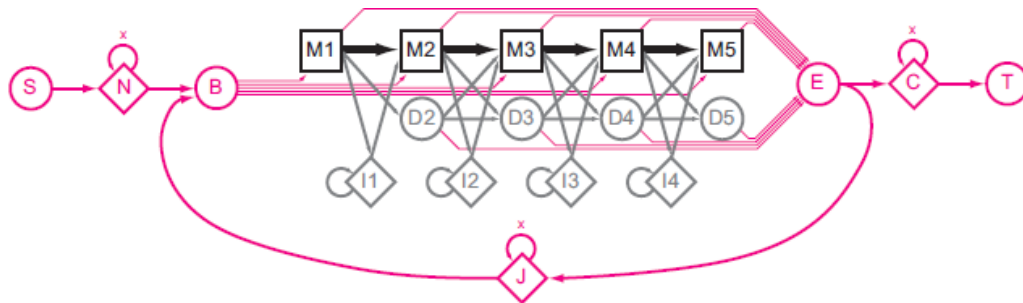
FIGURE 2.2: Profile HMM architecture used by HMMER(Eddy, 2011).

The structure begins at Start(S), and follows some chain of arrows until arriving at Termination(T). Each arrow transits to a state of the system. At each state, an action can be taken as either emitting a residue, or selecting an arrow to the next state. The actions are governed by a set of probabilities[Lesk, 2008]. The linear core model has five sets of match (M), insert (I) and delete (D) states. Each M state represents one consensus position. A set of M, I and D state is the main element of the model and is referred to as a "node" in HMMER. Additional flanking states (marked as N, C, and J) emit zero or more residues from the background distribution, modelling nonhomologous regions which precede, follow or join homologous regions. Start (S), begin (B), end (E) and termination (T) states are non-emitting states [Eddy, 2011].

A profile HMM for a protein family can be used to compare with target sequences, and classify sequences that are members of the family and those which are not[Eidhammer et al., 2004]. A common application of profile HMMs is used to search a profile HMM against a sequence database. Another application is the query of a single protein sequence of interest against a database of profile HMMs.

2.2.2.2 Viterbi algorithm in HMMER2

In HMMER2, both *hmmsearch* and *hmmpfam* rely on the same core Viterbi algorithm for their scoring function which is named as *P7Viterbi* in the codes.

To find whether a sequence is member of the family described by a HMM, we compare the sequence with the HMM. We use an algorithm known as the Viterbi algorithm to find one path that has the maximum probability of the HMM generating the sequence. The Viterbi algorithm is a dynamic programming algorithm. Let $V_{i,j}$ be the maximum probability of a path from the start state S_i ending at state S_j and generating the prefix $q_{1...j}$ of the target sequence. $V_{i+1,j}$ is found by the recurrence:

$$V_{i+1,j} = \max_{0 \leqslant k \leqslant j-1} \big(V_{i,k} P(k,j) P(q_{i+1}|j) \big)$$

Define $a[i,j]$ as the transition probability from state i to j and e_i as emission probability in state i. Define $V_j^M(i)$ as the log-odds score of the optimal path matching subsequence $x_{1...i}$ to the submodel up to state j, ending with x_i being emitted by *match* state M_j. Similarly $V_j^I(i)$ is the score of the optimal path ending in x_i being emitted by *insert* state I_j, and $V_j^D(i)$ for the optimal path ending in *delete* state D_j. Let q_{x_i} be the probability of x_i. Then we can write the Viterbi general equation[Durbin et al., 1998]:

$$V_j^M(i) = \log \frac{e_{M_j}(x_i)}{q_{x_i}} + max \begin{cases} V_{j-1}^M(i-1) + \log a[M_{j-1}, M_j] \\ V_{j-1}^I(i-1) + \log a[I_{j-1}, M_j] \\ V_{j-1}^D(i-1) + \log a[D_{j-1}, M_j] \end{cases}$$

$$V_j^I(i) = \log \frac{e_{I_j}(x_i)}{q_{x_i}} + max \begin{cases} V_j^M(i-1) + \log a[M_j, I_j] \\ V_j^I(i-1) + \log a[I_j, I_j] \end{cases}$$

$$V_j^D(i) = max \begin{cases} V_{j-1}^M(i) + \log a[M_{j-1}, D_j] \\ V_{j-1}^D(i) + \log a[D_{j-1}, D_j] \end{cases}$$

Based on the above equations, we can write the efficient pseudo code of the Viterbi algorithm, as shown in Algorithm 1 [Isa et al., 2012]. The inner loop of the code contains three two dimensional matrices (M, I, D), which calculate scores of all node positions involved in the main models for each of the residue. The outer loop consists of flanking and special states calculated in the one dimensional arrays N, B, C, J, E.

Algorithm 1 Pseudo code of the Viterbi algorithm

1: **procedure** VITERBI( )
2:     $N[0] \leftarrow 0; \quad B[0] \leftarrow tr(N, B)$
3:     $E[0] \leftarrow C[0] \leftarrow J[0] \leftarrow -\infty$
4:     **for** $i \leftarrow 1, L_t$ **do**   ▷ For every sequence residue i
5:         $N[i] \leftarrow N[i-1] + tr(N, N)$
6:         $B[i] \leftarrow max \begin{cases} N[i-1] + tr(N, B) \\ J[i-1] + tr(J, B) \end{cases}$
7:         $M[i, 0] \leftarrow I[i, 0] \leftarrow D[i, 0] \leftarrow -\infty$
8:         **for** $j \leftarrow 1, L_q$ **do**   ▷ For every model position j from 1 to L_q
9:             $M[0, j] \leftarrow I[0, j] \leftarrow D[0, j] \leftarrow -\infty$
10:             $M[i, j] \leftarrow e(M_j, S[i]) + max \begin{cases} M[i-1, j-1] + tr(M_{j-1}, M_j) \\ I[i-1, j-1] + tr(I_{j-1}, M_j) \\ D[i-1, j-1] + tr(D_{j-1}, M_j) \\ B[i-1] + tr(B, M_j) \end{cases}$
11:             $I[i, j] \leftarrow e(I_j, S[i]) + max \begin{cases} M[i-1, j] + tr(M_j, I_j) \\ I[i-1, j] + tr(I_j, I_j) \end{cases}$
12:             $D[i, j] \leftarrow max \begin{cases} M[i, j-1] + tr(M_{j-1}, D_j) \\ D[i, j-1] + tr(D_{j-1}, D_j) \end{cases}$
13:         **end for**
14:         $E[i] \leftarrow max\{M[i, j] + tr(M_j, E)\} \quad (j \leftarrow 0, L_q)$
15:         $J[i] \leftarrow max \begin{cases} J[i-1] + tr(J, J) \\ E[i-1] + tr(E, J) \end{cases}$
16:         $C[i] \leftarrow max \begin{cases} C[i-1] + tr(C, C) \\ E[i-1] + tr(E, C) \end{cases}$
17:     **end for**
18:     $Score \leftarrow C[L_t] + tr(C, T)$
19:     **return** $Score$
20: **end procedure**

From Algorithm 1, we can see the fundamental task of the Viterbi algorithm for biological sequence alignment is to calculate three DP(Dynamic Programming) matrices: $M[\ ]$ for

Match state, $I[\ ]$ for Insert state and $D[\ ]$ for Delete state. Each DP matrix consisting of $(L_t+1)*(L_q+1)$ blocks, where each value of block is dependent on the value of previous block. As shown in Figure 2.3, the Match state $M[i,j]$ depends on the upper-left block $M[i-1,j-1]$, $I[i-1,j-1]$ and $D[i-1,j-1]$; the Insert state $I[i,j]$ depends on the left block $M[i-1,j]$ and $I[i-1,j]$; and the Delete state depends on the upper block $M[i,j-1]$ and $D[i,j-1]$.
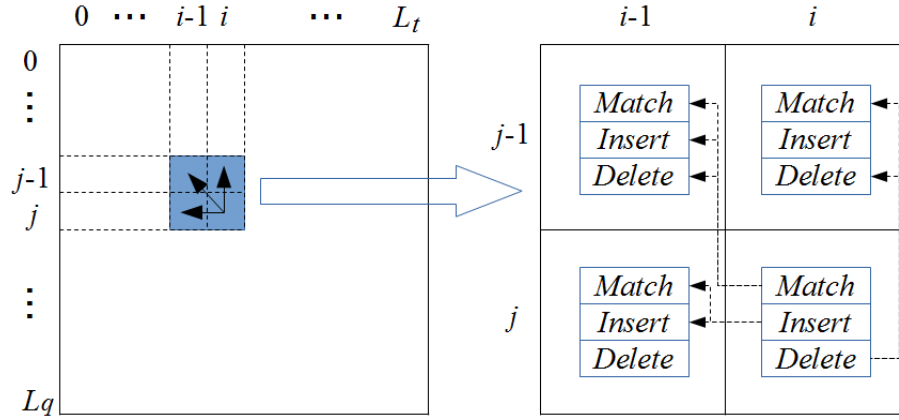
FIGURE 2.3: **The DP matrix calculated in Viterbi algorithm.** The rectangle on the left represents the whole matrix to be calculated by the Viterbi algorithm, and the right rectangle of the figure shows the process of updating a single block of the matrix.

2.2.2.3   MSV algorithm in HMMER3

HMMER3 is nearly total rewrite of the earlier HMMER2 package, with the aim of improving the speed of profile HMM searches. The main performance gain is due to a heuristic algorithm called the MSV filter, for Multiple (local, ungapped) Segment Viterbi. MSV is implemented in SIMD (Single-Instruction Multiple-Data) vector parallelization instructions and is about 100-fold faster than HMMER2.
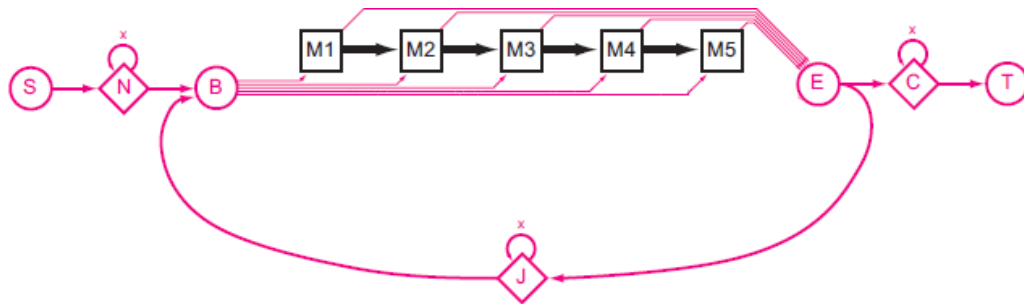
FIGURE 2.4: MSV profile: multiple ungapped local alignment segments (Eddy, 2011).

Figure 2.4 illustrates the MSV profile architecture. Compared with Figure 2.2, the MSV corresponds to the virtual removal of the delete and insert states. All match-match transition probabilities are treated as 1.0. The other parameters remains unchanged. So this model generates sequences containing one or more ungapped local alignment segments. The pseudo code of the MSV score algorithm is simplified and shown in Algorithm 2.

Algorithm 2 Pseudo code of the MSV algorithm

1: **procedure** MSV( )
2:     $N[0] \leftarrow 0; \quad B[0] \leftarrow tr(N, B)$
3:     $E[0] \leftarrow C[0] \leftarrow J[0] \leftarrow -\infty$
4:     **for** $i \leftarrow 1, L_t$ **do**   ▷ For every sequence residue i
5:         $N[i] \leftarrow N[i-1] + tr(N, N)$
6:         $B[i] \leftarrow max \begin{cases} N[i-1] + tr(N, B) \\ J[i-1] + tr(J, B) \end{cases}$
7:         $M[i, 0] \leftarrow -\infty$
8:         **for** $j \leftarrow 1, L_q$ **do**   ▷ For every model position j from 1 to L_q
9:             $M[0, j] \leftarrow -\infty$
10:             $M[i, j] \leftarrow e(M_j, S[i]) + max \begin{cases} M[i-1, j-1] \\ B[i-1] + tr(B, M_j) \end{cases}$
11:         **end for**
12:         $E[i] \leftarrow max\{M[i, j] + tr(M_j, E)\} \quad (j \leftarrow 0, L_q)$
13:         $J[i] \leftarrow max \begin{cases} J[i-1] + tr(J, J) \\ E[i-1] + tr(E, J) \end{cases}$
14:         $C[i] \leftarrow max \begin{cases} C[i-1] + tr(C, C) \\ E[i-1] + tr(E, C) \end{cases}$
15:     **end for**
16:     $Score \leftarrow C[L_t] + tr(C, T)$
17:     **return** $Score$
18: **end procedure**

Figure 2.5 illustrates an example of an alignment of a MSV profile HMM model (length $L_q = 14$) to a target sequence (length $L_t = 22$). A path to generate the target sequence with the profile HMM model is shown through a dynamic programming (DP) matrix. The model identifies two high-scoring ungapped alignment segments, as shown in black dots, indicating residues aligned to profile match states. All other residues are assigned to N, J, and C states in the model, as shown in orange dots. An unfilled dot indicates a "mute" non-emitting state or state transition.
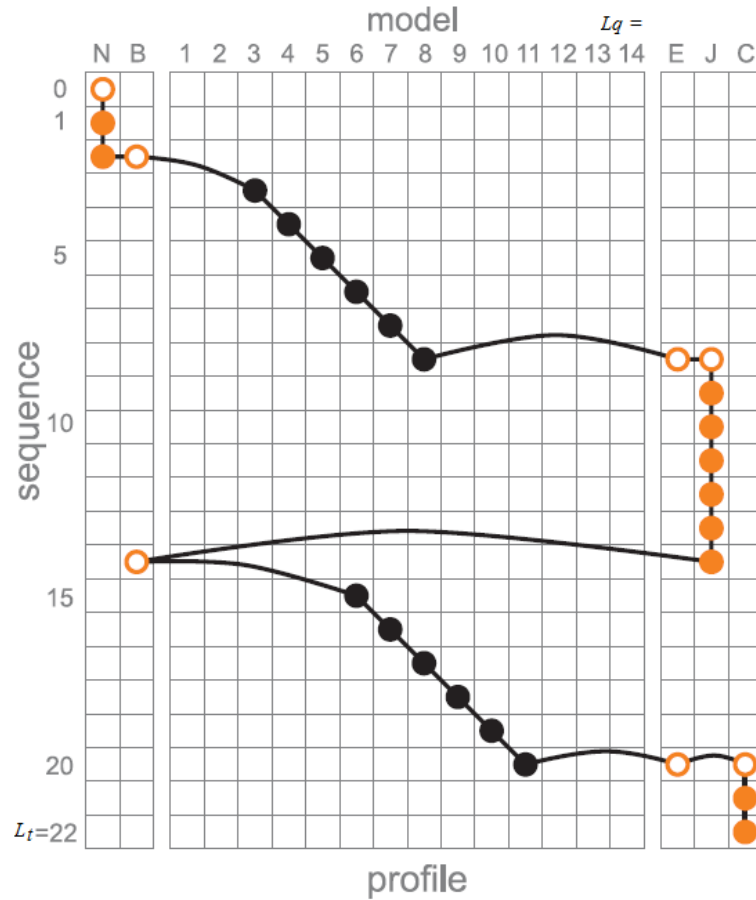
FIGURE 2.5: **Example of an MSV path in DP matrix (Eddy, 2011).** An alignment of a MSV profile HMM model (length $L_q = 14$) to a target sequence (length $L_t = 22$). A path from top to bottom is through a dynamic programming (DP) matrix. The model identifies two high-scoring ungapped alignment segments, as shown in black dots, indicating residues aligned to profile match states. All other residues are assigned to N, J, and C states in the model, as shown in orange dots. An unfilled dot indicates a "mute" non-emitting state or state transition.

2.2.2.4 SIMD vectorized MSV in HMMER3

A Single-Instruction Multiple-Data (SIMD) instruction is able to perform the same operation on multiple pieces of data in parallel. The first widely-deployed desktop SIMD implementation was with Intel's MMX extensions to the x86 architecture in 1996. In 1999, Intel introduced Streaming SIMD Extensions (SSE) in Pentium III series processors. The modern SIMD vector instruction sets use 128-bit vector registers to compute up to 16 simultaneous operations. Due to the huge number of iterations in the Smith-Waterman algorithm calculation, using SIMD instructions to reduce the number of instructions needed to perform one cell calculation has a significant impact on the

execution time. Several SIMD vector parallelization methods have been described for accelerating SW dynamic programming.

In 2000, Rognes and Seeberg presented an implementation of the SW algorithm running on the Intel Pentium processor using the MMX SIMD instructions [Rognes and Seeberg, 2000]. They used a query profile parallel to the query sequence for each possible residue. A query profile was pre-calculated in a sequential layout just once before searching the database. A six-fold speedup was reported over an optimized non-SIMD implementation.

In 2007, Farrar presented an efficient vector-parallel approach called stripped layout for vectorizing SW algorithm [Farrar, 2007]. He designed a stripped query profile for SIMD vector computation. He used Intel SSE2 to implement his design. A speedup of 2-8 times was reported over the Rognes and Seeberg SIMD non-stripped implementations.

Inspired by Farrar, in HMMER3 [Eddy, 2011], Sean R. Eddy used a remarkably efficient stripped vector-parallel approach to calculate the MSV alignment scores. To maximize parallelism, he implemented the MSV algorithm as a 16-fold parallel calculation with score values stored as 8-bit byte integers. He used SSE2 instructions on Intel-compatible systems and Altivec/VMX instructions on PowerPC systems.

Figure 2.6 shows the stripped and row-vectorized pattern in the implementation of the MSV algorithm in HMMER3. Each row of the dynamic programming matrix dp is divided into vectors with equal length L_v. The vector length L_v is equal to the number of elements being processed in the 128-bit SIMD register. Since the implementation processes 8-bit integers in parallel using SSE2 instructions, $L_v = 128/8 = 16$. The row length of the dp (i.e. the column number of the dp) is equal to the query profile HMM of length L. Hence, the number of vectors $L_Q = (L + L_v - 1)/L_v$. In Figure 2.6, we assume $L_v = 4, L = 14$, and $L_Q = 4$ for the simple illustration. The vectors are indexed by $q = 1...L_Q$ shown on the top of each vector. The cells of each row are aligned in a non-sequential stripped pattern and indexed by j. In the stripped pattern, the cells of the qth vector are indexed as $j = q, q + L_Q, q + 2L_Q, ..., q + (L_v - 1)L_Q$. For example, the 2nd vector has the cells $j = 2, 6, 10, 14$. Two unused cells at the end of the last two vectors are marked as $\times$ and set to a sentinel value.

In dynamic programming of the Smith-Waterman algorithm and the Viterbi algorithm, the calculation of each cell (i, j) in the dp is dependent on previously calculated cells
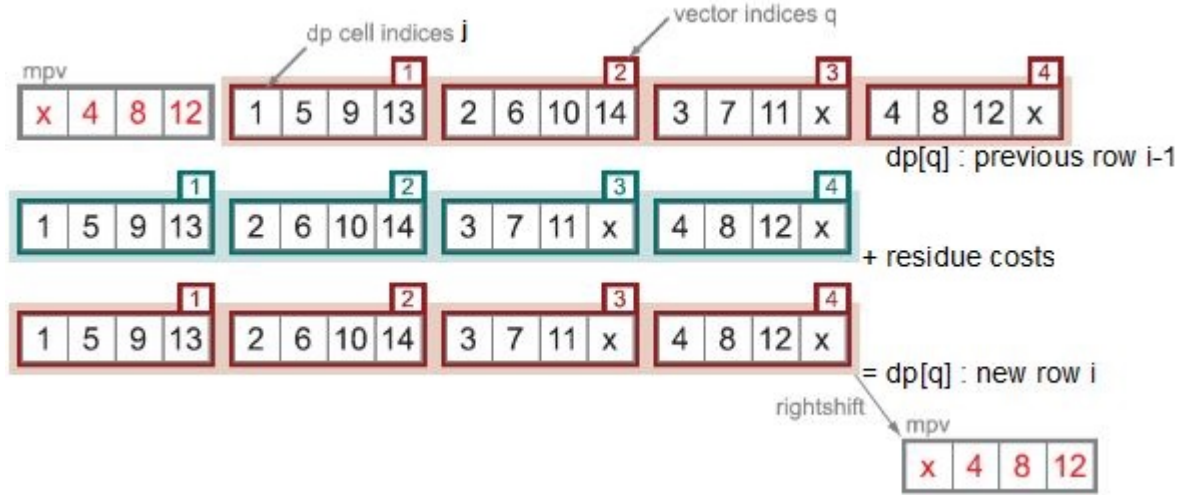
FIGURE 2.6: **Illustration of stripped indexing for SIMD vector calculations(Eddy, 2011)**. Each row of the dynamic programming matrix dp is row-vectorized and aligned in a stripped pattern. With the striped indexing, vector $q - 1$ in the top row contains exactly the four $j - 1$ cells, which are needed to calculate the four cells j in a new vector q in the middle row of the dp array. After calculating, the results are saved in the same dp array which is shown in the new bottom row. To calculate the first vector for the cells $j = (1, 5, 9, 13)$, we need the values of the cells ($\times$,4,8,12). We right-shift the last vector with $q = 4$ on each finished row and store the values of the cells ($\times$,4,8,12) in the vector mpv.

$(i - 1, j), (i, j - 1)$ and $(i - 1, j - 1)$. However, in the MSV algorithm, the *delete* and *insert* states have been removed and only ungapped diagonals need calculating, so the calculation of each cell (i, j) requires only previous $(i - 1, j - 1)$. In Figure 2.6, the top red row shows the previous row $i - 1$ for the cells $j - 1$, which is needed for calculating each new cell j in a new row i.

The striping method can remove the SIMD register data dependencies. In the Figure 2.6, with the striped indexing, vector $q - 1$ in the top row contains exactly the four $j - 1$ cells, which are needed to calculate the four cells j in a new vector q in the middle row of the dp array. For example, when we calculate cells $j = (2, 6, 10, 14)$ in vector $q = 2$ in the middle row, we access the previous row's vector $q - 1 = 1$ which contains the cells we need in the order we need them, $j - 1 = (1, 5, 9, 13)$ (the vector above). After calculating, we save the results in the same dp array which is shown in the new bottom row.

To calculate the first vector with $q = 1$ for the cells $j = (1, 5, 9, 13)$, we need the values of the cells ($\times$,4,8,12). Because the first cell $j = 1$ is not dependent on any previous cell, we indicate its dependency cell as $\times$. To fetch the values of the cells ($\times$,4,8,12), we

right-shift the last vector with $q = 4$ on each finished row and store the values in the vector mpv. The mpv is used to initialize the next row calculation.
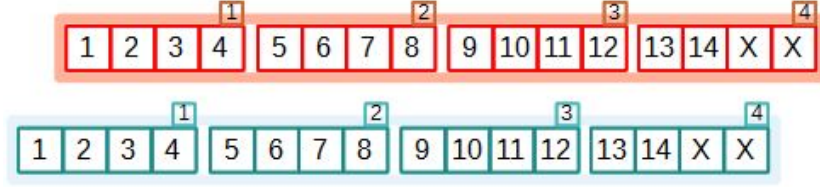
FIGURE 2.7: Illustration of linear indexing for SIMD vector calculations.

Instead, if we indexed cells into vectors in the linear order ($j = 1, 2, 3, 4$ in vector $q = 1$ and so on), as shown in Figure 2.7, there is no such correspondence of $(q, q-1)$ with four $(j-1, j)$, and each calculation of a new vector q would require extra expensive operations, such as shifting or rearranging cell values inside the previous row's vectors. By using the stripped query access, only one shift operation is needed per row as shown in Figure 2.6.

The pseudo code for the implementation is shown in Algorithm 3

Algorithm 3 Pseudo code of the SIMD vectorized MSV algorithm

1: **procedure** MSV-SIMD( )
2:   $xJ \leftarrow 0; \quad dp[q] \leftarrow vec\_splat(0) \ (q \leftarrow 0, L_Q - 1)$
3:   $xB \leftarrow base + tr(N, B)$
4:   $xBv \leftarrow vec\_adds(xB, tr(B, M))$
5:   **for** $i \leftarrow 1, L_t$ **do**   ▷ For every sequence residue i
6:     $xEv \leftarrow vec\_splat(0)$
7:     $mpv \leftarrow vec\_rightshift(dp[L_Q - 1])$
8:     **for** $q \leftarrow 0, L_Q - 1$ **do**
9:       $tmpv \leftarrow vec\_max(mpv, xBv)$ ▷ temporary storage of 1 current row value
10:      $tmpv \leftarrow vec\_adds(tmpv, e(M_j, S[i]))$
11:      $xEv \leftarrow vec\_max(xEv, tmpv)$
12:      $mpv \leftarrow dp[q]$
13:      $dp[q] \leftarrow tmpv$
14:     **end for**
15:    $xE \leftarrow vec\_hmax(xEv)$
16:    $xJ \leftarrow max \begin{cases} xJ \\ xE + tr(E, J) \end{cases}$
17:    $xB \leftarrow max \begin{cases} base \\ xJ + tr(J, B) \end{cases}$
18:   **end for**
19:   $Score \leftarrow xJ + tr(C, T)$
20:   **return** $Score$
21: **end procedure**

Five pseudocode vector instructions for operations on 8-bit integers are used in the pseudo code. The instructions are vec_splat, vec_adds, vec_rightshift, vec_max and vec_hmax. Either scalars x or vectors v containing 16 8-bit integer elements numbered $v[0]...v[15]$. Each of these operations are either available or easily constructed in Intel SSE2 intrinsics as shown in Table 2.2.

Pseudocode SSE2 intrinsic in C	Operation	Definition
v = vec_splat(x) v = _mm_set1_epi8(x)	assignment	$v[z] = x$
v = vec_adds(v1, v2) v = _mm_adds_epu8(v1, v2)	saturated addition	$v[z] = min \begin{cases} 2^8 - 1 \\ v1[z] + v2[z] \end{cases}$
v1 = vec_rightshift(v2) v1 = _mm_slli_si128(v2, 1)	right shift	$v1[z] = v2[z-1](z = 15...1);$ $v1[0] = 0;$
v = vec_max(v1, v2) v = _mm_max_epu8(v1, v2)	max	$v[z] = max(v1[z], v2[z])$
x = vec_hmax(v) -	horizontal max	$x = max(v[z]), z = 0...15$

TABLE 2.2: **SSE2 intrinsics for pseudocode in Algorithm 3** The first column is pseudocode and its corresponding SSE2 intrinsic in C language. Because x86 and x86-64 use little endian, **vec_rightshift()** means using a left bit shift intrinsic **_mm_slli_si128()** to do right shift. No SSE2 intrinsic is corresponding to **vec_hmax()**. Shuffle intrinsic **_mm_shuffle_epi32** and **_mm_max_epu8** can be combined to implement **vec_hmax()**.

2.3 CUDA accelerated sequence alignment

In November 2006, NVIDIA introduced CUDA (Compute Unified Device Architecture), a general purpose parallel computing platform and programming model that enables users to write scalable multi-threaded programs in NVIDIA GPUs. Nowadays there exist alternatives to CUDA, such as OpenCL [OpenCL, 2014], Microsoft Compute Shader[Microsoft, 2013-11]. These are similar, but as CUDA is the most widely used and more mature, this thesis will focus on that.

This section overviews CUDA programming model, then reviews recent studies on accelerating Smith-waterman algorithm and HMM-based algorithms on CUDA-enabled GPU.

2.3.1 Overview of CUDA programming model

2.3.1.1 Streaming Multiprocessors

A GPU consists of one or more SMs (Streaming Multiprocessors). Quadro K4000 used in our research has 4 SMs. Each SM contains the following specific features [Wilt, 2013]:

- Execution units to perform integer and single- or double-precision floating-point arithmetic, special function units to compute single-precision floating-point transcendental functions

- Thousands of registers to be partitioned among threads

- Shared memory for fast data interchange between threads

- Several caches, including constant cache, texture cache and L1 cache

- A warp scheduler to coordinate instruction dispatch to the execution units

The SM has been evolving rapidly since the introduction of the first CUDA-enabled GPU device in 2006, with three major Compute Capability 1.x, 2.x, and 3.x, corresponding to Tesla-class, Fermi-class, and Kepler-class hardware respectively. Table 2.3 summarizes the features introduced in each generation of the SM hardware [Wilt, 2013].

Compute Capability	Features introduced
SM 1.x	Global memory atomics; mapped pinned memory; debuggable; atomic operations on shared memory; Double precision
SM 2.x	64-bit addressing; L1 and L2 cache; concurrent kernel execution; global atomic add for single-precision floating-point values; Function calls and indirect calls in kernels
SM 3.x	SIMD Video Instructions; Increase maximum grid size; warp shuffle; Bindless textures ("texture objects"); read global memory via texture; faster global atomics; 64-bit atomic min, max, AND, OR, and XOR; dynamic parallelism

TABLE 2.3: Features per Compute Capability

2.3.1.2 CUDA thread hierarchy

The execution of a typical CUDA program is illustrated in Figure 2.8 The CPU host invokes a GPU kernel in-line with the triple angle-bracket $<<<$ $>>>$ syntax from

CUDA C/C++ extension code. The kernel is executed N times in parallel by N different CUDA threads. All the threads that are generated by a kernel during an invocation are collectively called a *grid*. Figure 2.8 shows the execution of two grids of threads.
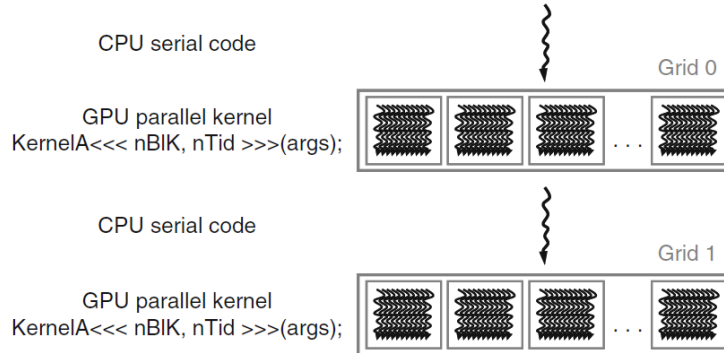
FIGURE 2.8: Execution of a CUDA program(Kirk and Hwu, 2010).

Threads in a grid are organized into a two-level hierarchy, as illustrated in Figure 2.9. At the top level, each grid consists of one or more thread blocks. All blocks in a grid have the same number of threads and are organized into a one-, two-, or three-dimensional *grid* of thread blocks.
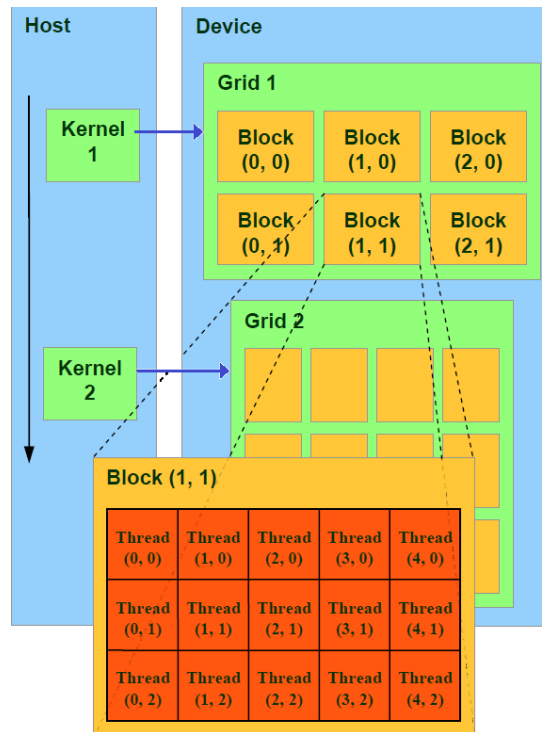
FIGURE 2.9: CUDA thread organization(Zeller, 2008).

Each block can be identified by an index accessible within the kernel through the built-in *blockIdx* variable. The dimension of the thread block is accessible within the kernel

through the built-in *blockDim* variable.

The threads in a block are executed by the same multiprocessor within a GPU. They can cooperate by sharing data through some shared memory and by synchronizing their execution to coordinate memory accesses. Each block can be scheduled on any of the available multiprocessors, in any order, concurrently or sequentially, so that a compiled CUDA program can execute on any number of multiprocessors. On the hardware level, a block's threads are executed in parallel as *warps*. The name warp originates from *weaving loom*. A warp consists of 32 threads.

2.3.1.3   CUDA memory hierarchy

Besides the threading model, another thing that makes CUDA programming different from a general purpose CPU is its memory spaces, including registers, local, shared, global, constant and texture memory, as shown in Figure 2.10.
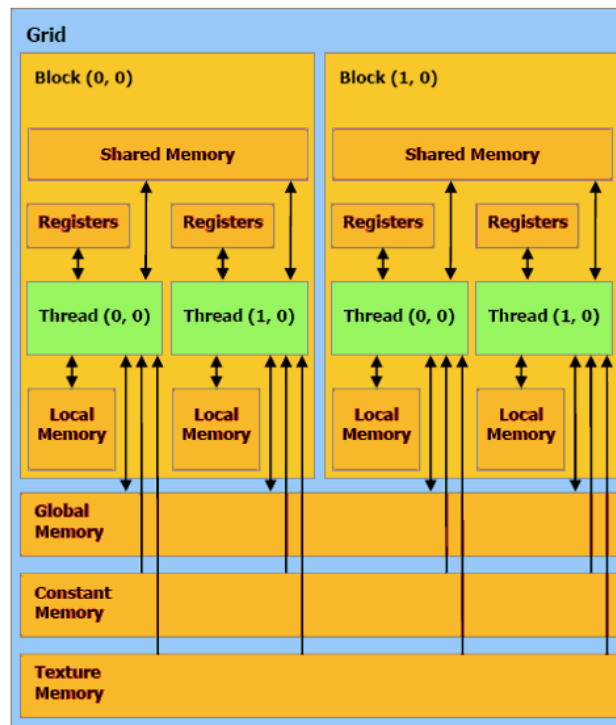
FIGURE 2.10: CUDA memory organization(Zeller, 2008).

CUDA memory spaces have different characteristics that reflect their distinct usages in CUDA applications as summarized in Table 2.4 [NVIDIA, 2013-07a]. The texture, contant and global memory can be allocated by CPU host. Shared memory can only be shared and accessed by threads in a block. Registers and local memory are only

available for one thread. Register access is the fastest and global memory access is the slowest. Since these memories have different features, one important thing of CUDA programming is how to combine these memories to best suit the application.

Memory	Location	Cached	Access	Scope	Speed	Lifetime
Register	On chip	n/a	R/W	1 Thread	1	Thread
Local	Off chip	†	R/W	1 Thread	$\sim 2 - 16$	Thread
Shared	On chip	n/a	R/W	All threads in block	$\sim 2 - 16$	Block
Global	Off chip	†	R/W	All threads + host	200+	Host allocation
Constant	Off chip	Yes	R	All threads + host	$2 - 200$	Host allocation
Texture	Off chip	Yes	R	All threads + host	$2 - 200$	Host allocation

TABLE 2.4: **Salient Features of GPU Device Memory. Speed** column is the relative speed in number of instructions. † means it is cached only on devices of above compute capability 2.x.

2.3.1.4 CUDA tools

The NVIDIA CUDA Toolkit provides a comprehensive development environment for C/C++ developers building GPU-accelerated applications. The CUDA Toolkit is available at https://developer.nvidia.com/cuda-toolkit, including a compiler *nvcc* for NVIDIA GPUs, math libraries, and tools for debugging and optimizing the performance of CUDA applications.

Nsight Eclipse Edition

NVIDIA Nsight Eclipse Edition is a full-featured IDE powered by the Eclipse platform that provides an all-in-one integrated programming environment for editing, building, debugging and profiling CUDA C/C++ applications. Nsight Eclipse Edition supports a rich set of commercial and free plugins. Nsight Eclipse Edition ships as part of the CUDA Toolkit Installer for Linux and Mac at https://developer.nvidia.com/nsight-eclipse-edition.

NVIDIA Nsight Visual Studio Edition

NVIDIA provides Nsight Visual Studio Edition to integrate seamlessly into Microsoft Visual Studio environment. It can build, debug, profile and trace heterogeneous compute

and graphics applications using CUDA C/C++, OpenCL [OpenCL, 2014], DirectCompute [Microsoft, 2013-11], Direct3D, and OpenGL.

Profiling tools

NVIDIA provides profiling tools to execute the kernels in question under instrumentation, which are publicly available as a separate download on the CUDA Zone website [NVIDIA, 2014b].

Tools Name	OS	User interface
nvprof	Linux, Mac OS X and Windows	command-line
Visual Profiler	Linux, Mac OS X and Windows	graphical
Nsight Ecipse Edition	Linux and Mac OSX	graphical
NVIDIA Nsight Visual Studio Edition	Windows	graphical
Parallel Nsight	Windows	graphical

TABLE 2.5: CUDA profiling tools

Nvidia-SMI

The NVIDIA System Management Interface (nvidia-smi) is a command line utility that manages and monitors GPU devices. It ships with NVIDIA GPU display drivers on Linux and Windows. This utility allows administrators to query the GPU device state and modify the GPU device state. It can also report control aspects of GPU execution, such as whether ECC (Error Checking and Correction) is enabled and how many CUDA contexts can be created on a given GPU.

2.3.2 CUDA accelerated Smith-Waterman

The Smith-Waterman algorithm exploits dynamic programming for sequence alignment, which is also the characteristic of the HMM-based algorithms. In this section, we review the techniques used in parallelizing Smith-Waterman on a CUDA-enabled GPU and these techniques will be evaluated for accelerating the MSV algorithm in Chapter 3.

Parallelism strategy applied

1) Task-based parallelism

As explained in Section 3.1, parallel computing has two types of parallelism: task-based and data-based parallelism. The SW algorithm is used for finding similarity among protein sequence database with dynamic programming. The application is particularly well-suited for many-core architectures due to the parallel nature of sequence database searches.

Liu et al. have been accelerating Smith-Waterman sequence database searches for CUDA-enabled GPU since 2009. Here are their 3 articles from 2009 to 2013: [Liu et al., 2009], [Liu et al., 2010] and [Liu et al., 2013]. They present many approaches for optimization. They use task-based parallelism to process each target sequence independently with a single GPU thread. Task-based parallelism removes the need for inter-thread communications or, even worse, inter-multiprocessor communications. This also simplifies implementation and testing.

Due to these reasons, task-based parallelism has been taken by most of studies and more efforts are put on optimizing CUDA kernel execution. Among 8 articles reviewed here, 7 articles apply this approach. Beside 3 articles of Liu et al., other 4 article are [Manavski, 2008], [Akoglu and Striemer, 2009], [Ligowski and Rudnicki, 2009] and [Kentie, 2010].

[Liu et al., 2013] not only distributes tasks to many threads in the GPU kernel, but also balances the workload between the CPU and the GPU. Their distribution policy calculates a rate R of the number of residues from the database assigned to GPUs, with a formular as

$$R = \frac{N_G f_G}{N_G f_G + N_C f_C / C}$$

where f_C and f_G are the core frequencies of the CPU and the GPU respectively, N_C and N_G are the number of CPU cores and the number of GPU SMs respectively, and C is a constant derived from empirical evaluations.

They find the sequence length deviation generally causes execution imbalance between threads, which in return can not fully utilize the GPU compute power. Considering this, they design two CUDA kernels based on two parallelization approaches: static scheduling and dynamic scheduling. These two kernels are launched based on the sequence length deviation of the database.

Since each thread has its own buffers in global memory, the static scheduling launches all thread blocks onto the GPU at the same time. When a thread block finishes its current computation, this thread block will use the dynamic scheduling to obtain an unprocessed profile block. They use the atomic addition function *atomicAdd*() to increment the index of global profile blocks.

[Manavski, 2008] also distributes some tasks to the CPU. In the GPU, they only launch 450 thread-blocks at a time on a grid. For a database with more than 450 sequences, several kernel launches are necessary and this will create additional latency. Since they run 64 threads per block, they can only process 450 * 64 = 28,800 alignments per kernel launch. CUDA limits the number of blocks in a grid to 65,535 blocks in a single dimension, which is far above their threshold. This results in low GPU kernel thread occupancy.

Considering Manavski's implementation limitation in thread occupancy, [Akoglu and Striemer, 2009] sets thread block size by the total number of sequences in the database so that they can to do all alignments with a single kernel launch.

In order to achieve high efficiency for task-based parallelism, the run time of all threads in a thread block should be roughly identical. Therefore many studies often sort sequence databases by the length of the sequences. Thus, for two adjacent threads in a thread warp, the difference between the lengths of the associated sequences is minimized, thereby balancing a similar workload over threads in a warp.

[Manavski, 2008], [Akoglu and Striemer, 2009], [Liu et al., 2009], [Liu et al., 2010] and [Liu et al., 2013] use a presorted database in ascending order.

[Ligowski and Rudnicki, 2009] presorts the database in descending order and organizes data in blocks consisting of 256 sequences, since each kernel has 16 blocks, and a single block consists of 256 threads. The choice of 4096 threads per kernel is dictated partially by limitations of architecture and partially by optimization of performance. There are 16 multiprocessors in each core, each executes a single block of threads. The number of 256 threads per block is limited by the number of registers (8192 per multiprocessor). The SW main routine needs 29 registers, and therefore the highest multiple of 64 that can be concurrently executed is 256. They process the alignment matrix horizontally. The main loop for calculating the matrix is executed for a band of 12 cell columns. Slow

global memory is accessed only at the initialization and termination of the loop. Fast shared memory and registers are used for all operations within the loop. The width of the band is limited by the availability of shared memory.

[Kentie, 2010] implements a *dbconv* tool to presort a database in descending order and converts the database into a special format. The *dbconv* writes the sorted sequences to file in an interlaced fashion: the database is split up into half-warp sized blocks of 16 sequences. The sequences of a block are written in an alternating fashion: one 8-bit symbol of the first sequence is written, then one of the second one, etc. In this way, the first character of all 16 sequences is written, then the second character, etc. All sequences in a rectangular block are padded to the length of the block's longest sequence with blank symbols. Hence, all of a half-warp's threads will load database symbols from neighboring addresses so as to access the global memory in a coalesced way.

2) Data-based parallelism

In data-based parallelism, each task is assigned to one or many thread block(s) and all threads in the thread block(s) cooperate to perform the task in parallel.

The main target of [Saeed et al., 2010] is to solve a single but very large Smith-Waterman problem for sequences with very long lengths. Their calculation works along anti-diagonals of the alignment matrix. Each diagonal item can be calculated independently of the others. Block diagonal algorithms are also possible as long as each block is processed serially.

They formulate a parallel version of the Smith-Waterman algorithm so that the calculations can be performed in parallel one row (or column) of the similarity matrix at a time. Row (or column) calculations allow the GPU global memory accesses to be consecutive and therefore high memory throughput is achieved.

They exploit this approach of parallelizing a single GPU by using MPI (Message Passing Interface) over 100 Mb Ethernet to extend work to multiple GPUs. To use N GPUs, the Smith-Waterman alignment matrix is decomposed into N large, and slightly overlapping blocks.

[Liu et al., 2009] investigate the two parallelism approaches for parallelizing the sequence database searches using CUDA. They find task-based parallelism can achieve better performance although it needs more device memory than data-based parallelism. For

task-based parallelism, they sort target sequences and store them in an array row by row from the top-left corner to the bottom-right corner, where all symbols of a sequence are restricted to be stored in the same row from left to right. Using these arrangement patterns for the two parallelism strategies, access to the target sequences is coalesced for all threads in a half-warp.

To maximize performance and to reduce the bandwidth demand of global memory, they also apply a cell block division method for the task-based parallelism, where the alignment matrix is divided into cell blocks of equal size.

They apply data-based parallelism to support longest query/target sequences. Each task is assigned to one thread block and all threads in the thread block cooperate to perform the task in parallel, exploiting the parallel characteristics of cells in the minor diagonals of the similarity matrix.

Device memory access pattern

As described in Section 2.3.1.3, CUDA memory hierarchy includes registers, local, shared, global, constant and texture memory, as shown in Figure 2.10. Memory throughput generally dominates program performance both in the CPU and GPU domains. Here is a review of how these studies applied different device memory access pattern to optimize their implementations.

[Liu et al., 2009] sorts target sequences and arranges them in an array like a multi-layer bookcase to store into global memory, so that the reading of the database across multiple threads could be coalesced. Writes to global memory are first batched in shared memory for better coalescing. Due to a reduction in the global memory accesses, they propose a cell block division method for the task-based parallelism, where the alignment matrix is divided into cell blocks of equal size. They utilize the texture memory on the sorted array of target sequences in order to achieve maximum performance on coalesced access patterns. They use a hash table to index the location coordinate in the array and the length of each sequence, which can provide fast access to any sequence.

They also exploit constant memory to store the gap penalties, scoring matrix and the query sequence. They load the scoring matrix into shared memory, as the performance of constant memory degrades linearly when threads frequently need to access multiple

different addresses in the scoring matrix. They also use the CUDA built-int integer functions max(x, y) and min(x, y) to improve performance further.

[Kentie, 2010] reduces global memory access by making temporary values interleaved and reads/writes score and temporary values in one access. Kentie exploits constant memory and shared memory for the substitution matrix. Constant memory is fast, but only if all threads read the same address. This is not suited to the substitution matrix. Shared memory has several disadvantages for the matrix. Finally, he finds texture memory has the ability to fetch four values at a time and is well suited for random access. He gains a total speedup of 25% after switching from shared memory to texture memory. He also stores gap penalties in constant memory.

[Akoglu and Striemer, 2009] stores database sequences in global memory. The cell calculation blocks are used to store temporary calculation values needed for data dependencies for each column and are also stored in global memory. They use the substitution matrix instead of the query profile to save memory size. In order to index the row and column of the matrix in extremely efficient way, they design a simple function for accessing the matrix, which is as follows:

$$S_{i,j} = (ascii(S_1) - 65, ascii(S_2) - 65)$$

where S_1 is a residue from the query sequence and S_2 is a residue from one of the database sequences. They map the query sequence as well as the substitution matrix to the constant memory to make access to these values easy. They track the highest SW score by a single register in the kernel for each thread, and update on each pass of the inner loop. Then the score is written to the global memory, after the alignment is finished.

Among the 7 articles reviewed here, [Manavski, 2008] is the first to study accelerating SW on CUDA-enabled GPU in 2007. They present the query profile as a query-specific substitution matrix computed only once for the entire database. They exploit the cache of texture memory to store query profiles. In this way they replace random accesses to the substitution matrix with sequential ones to the query profile.

[Liu et al., 2010] utilizes texture memory to store query profiles. They use shared memory to store the 4 residues of a target sequence.

[Liu et al., 2013] stores both the query profile and its variant in texture memory. They gain more performance from the query profile variant for short queries, because it can reduce the number of fetches from texture memory by half. However, for longer queries, a query profile becomes superior due to its much smaller memory footprint and fewer texture cache misses. They apply a query length threshold Q to decide whether to use the query profile or the variant.

[Ligowski and Rudnicki, 2009] reduces global memory access only at the loop initialization stage and for writing the results at the exit stage. They performed all operations within the loop in fast shared memory and registers.

Vector programming model

The vector programming model plays an important role in operations on array or matrix data structure. On one hand, it can reduce greatly the frequency of memory access; on the other hand, it can utilize the built-in SIMD vector instructions for parallel computing both on the CPU and the GPU.

[Manavski, 2008] packs the query profile in texture memory, storing 4 successive values into the 4 bytes of a single unsigned integer. To compute a column of the alignment matrix, all the H and E values are needed from the previous column. They place them in two local memory buffers of the thread: one for the previous values and another for the newly computed ones. At the end of processing each column, they swap the buffers. Since local memory is not cached, they use a specific access pattern to read 4 H and 4 E values from local memory at a time, which can fully take advantage of the 128-bit memory bandwidth. Thus, each thread can gather all the data needed to compute 4 cells of the alignment matrix with only two read instructions: one from the local buffer and another from the texture memory.

Manavski pre-computes a query profile of the query sequence for each possible residue and achieves dynamic load balancing between multiple GPUs according to their computational power at run time.

[Akoglu and Striemer, 2009] calculates the Smith-Waterman score from the query sequence and database sequences by means of columns, 4 cells at a time for the residue of database sequence aligned with an 8 residue query sequence. The updated values of cells

are placed in a temporary location in the global memory. This cell calculation block is updated each time a new column is computed, and is utilized for dependency purposes in computing columns on each pass.

[Liu et al., 2010] designs a stripped query profile for SIMD vector computation and uses a packed data format to store into the CUDA built-in *uchar4* vector data type, instead of the *char* scalar data type. In this way, 4 substitution scores can be accessed with only one fetch from texture memory, thus greatly improving texture memory throughput.

Like the query profile, they also construct each target sequence with a packed data format, where 4 successive residues of each target sequence are packed together and placed in a variable of type *uchar4*. In this case, they utilize shared memory to store the 4 residues loaded by one fetch from texture memory for the use of the inner loop, when using the cell block division method.

They use maximum and minimum operation to artificially implement saturation addition and saturation subtraction. The CUDA built-in integer functions max(x, y) and min(x, y) are utilized to avoid divergence. They implement a shift operation on a vector using shared memory, where all threads comprising a virtualized vector write their original values to a shared memory buffer and then read their resulting values from the buffer as per the number of shift elements.

They divide a query sequence into a series of non-overlapping, consecutive small partitions with a specified partition length, and then align the query sequence to a subject sequence partition by partition. They port the SIMD CPU algorithm [Farrar, 2007] to the GPU, viewing collections of processing elements as part of a single vector.

[Kentie, 2010] applies a vector data structure to load 4 query characters at a time and process 8 database characters at a time. He loads query profile values for the 4 current query characters and passes them to the Smith-Waterman function. The 4 query symbols and loaded query profile values are aligned with each loaded database symbol. He simplifies substitution matrix lookup by using numeric values instead of letters for sequence symbols.

[Liu et al., 2013] designs a query profile variant data structure and packs the 4 consecutive elements of variant data into the built-in *short4* vector type. In this way, although the variant data needs more memory space compared to the query profile, they can reduce

the number of fetches from texture memory for the variant by half. On the other hand, using the variant can save 6 bitwise operations for generating a substitution score vector. They also utilize the built-in *uint4* vector data type to store each sequence profile for quad-lane SIMD computing on GPUs.

They use the CUDA SIMD Video Instructions in GPU computing and use Intel SSE2 intrinsic in CPU computing. For the CPU SIMD computation, their approach is based on the open-source SWIPE software [Rognes, 2011]. They compute the SW algorithm by splitting an SSE vector to 16 lanes with 8-bit lane width. Then they re-compute all alignments, whose scores have overflow potential, using 8-lane SSE vectors with 16-bit lane width.

2.3.3 CUDA accelerated HMMER

HMMER includes a MPI (Message Passing Interface) implementation of the search algorithms, which uses conventional CPU clusters for parallel computing. ClawHMMer [Horn et al., 2005] is the first GPU-enabled *hmmsearch* implementation. Their implementation is based on the BrookGPU stream programming language, not the CUDA programming model. Since ClawHMMer, there has been several studies on accelerating HMMER for a CUDA-enabled GPU. The following is the summary of techniques applied by the research work.

Parallelism strategy applied

As explained in Section 3.1, parallel computing has two types of parallelism: task-based and data-based parallelism. SW algorithm is used for finding similarity among protein sequence database with dynamic programming method. The application is particularly well-suited for many-core architectures due to the parallel nature of sequence database searches. Among 5 articles reviewed here, 3 articles, i.e. [Walters et al., 2009], [Quirem et al., 2011] and [Ahmed et al., 2012] used task-based parallelism to process each target sequence independently with a single GPU thread. Task-based parallelism removes the need for inter-thread communications or, even worse, inter-multiprocessor communications. This also simplifies implementation and testing. This approach was taken by most of studies and more efforts were put on optimizing the CUDA kernel execution.

[Walters et al., 2009] ports the Viterbi function to a CUDA-enabled GPU with a variety of optimization approaches. Their implementation operates the GPU kernel on multiple sequences simultaneously, with each thread operating on an independent sequence. They found the number of threads that can be executed in parallel will be limited by two factors: one is the GPU memory which limits the number of sequences that can be stored, and another is the number of registers used by each thread which limits the number of threads that can execute in parallel. Registers are the most important resource in their implementation.

They split the inner loop for computing the dynamic programming matrix into three independent small loops. This approach requires fewer registers, resulting in higher GPU utilization. Further, splitting the loop provides an easy mechanism to exploit loop unrolling, which is a classic loop optimization strategy designed to reduce the overhead of inefficient looping. The idea is to replicate the loops inner contents such that the percentage of useful instructions in each statement of the loop increases. In their experiment, the performance improvement reaches 80%.

In order to achieve high efficiency for task-based parallelism, the run time of all threads in a thread block should be roughly identical. Therefore many studies often sort sequence databases by the length of the sequences. Thus, for two adjacent threads in a thread warp, the difference between the lengths of the associated sequences is minimized, thereby balancing a similar workload over threads in a warp. Walters et al. presort the sequence database in ascending order. This approach is both an effective and straightforward optimization and they gain a nearly 7x performance improvement over the unsorted database without changing the CUDA kernel in any way.

Walters et al. distribute some tasks to the CPU, creating two CPU threads, one thread for reading the database and one thread for post-processing the database hits.

For data-based parallelism, based on the *wave-front* method [Aji et al., 2008], [Du et al., 2010] applies a new tile-based mechanism to accelerate the Viterbi algorithm on a single GPU. The *wave-front* method computes the cells along the anti-diagonal of the dynamic matrix in parallel, which is similar to a frontier of a wave to fill a matrix, where each cell's value in the matrix is computed based on the values of the left, upper, and upper-left cells.

They apply a streaming method to process very long sequences. In CUDA, a stream is a set of instructions that execute in order. Different streams may execute their instructions asynchronously. This feature enables their execution to be overlapped with each other between the host and the GPU device.

Since the streaming Viterbi algorithm requires additional storage and communication bandwidth, they design the new tile-based method to simplify the computational model. The method also handles very long sequences with less memory transfer. The tile-based method handles very long sequence as follows: the large matrix is divided into tiles to ensure that each tile fits in the GPUs memory as a whole and computes the tiles in parallel. Unlike the tiling machanism in [Aji et al., 2008], which has data dependencies among each tile, they introduce the *homological segments* concept into their tile-based mechanism to eliminate the data dependency among different tiles. They apply the k-mer based algorithm to find all homological segments. Then the homological segments are used to divide the full dynamic programming matrix into small tiles.

[Ganesan et al., 2010] parallelizes the Viterbi algorithm to accelerate hmmsearch. They present a hybrid parallelization strategy by combining task-based and data-based parallelism. They extend the existing task parallelism upon which data parallelism is built. They reassign the computation of a single sequence across multiple threads to implement the data parallelism. In order to accelerate the computation of the dynamic programming matrix rows, they partition each row into equal sized intervals of contiguous cells and calculate the dependencies between the partitions identically and independently in a data parallel setting.

They process the parallel computation of the rows in three phases as follows:

1. Phase 1 uses independent threads to compute the relationship between the beginning and end of each partition, which enables the fast computation of boundary elements between the partitions.

2. Phase 2 applies the functions relating the boundary elements from Phase 1, to compute the numeric values for each of the boundary elements. This phase executes consecutively, with N partitions requiring N steps.

3. Phase 3 uses the updated numerical values for each of the boundary elements, so each partition independently computes the numeric values for all of the elements within the partition in the data parallelism setting.

Phase 1 is the critical phase that facilitates data parallelism by building the relationship among the different partitions. Phases 2 and 3 are computation phases for the boundary and internal elements of partitions respectively.

[Ganesan et al., 2010] implements the partitioning scheme by storing index data of the model positions at regular intervals consecutively to achieve coalesced global memory access. They benchmark the implementation on Tesla C1060, showing a speed-up of 5x-8x compared to [Walters et al., 2009] using an unsorted database.

[Ahmed et al., 2012] uses the Intel VTune Analyzer [Intel, 2013] to investigate performance hotspot functions in HMMER3. Based on hotspot analysis, they study CUDA acceleration for three individual algorithms: Forward, Backward and Viterbi algorithm. They found data transfer overhead between heterogeneous processors could be a performance bottleneck.

Based on their experiments, they show that the Forward, Backward and Viterbi function take 37%, 31% and 20% respectively for the percentage of the total CPU clock. They tested their CUDA implementation of these three functions. Their results show about 2.27x, 1.58x and 1.50x speedup over the original CPU-only implementation for the Forward, Backward and Viterbi function respectively. Since the Forward function uses the most time among the three functions, it is the most dominant module and the CUDA implementation of Forward has the largest impact on speedup. The Backward function has the second largest speedup and the Viterbi function has the least speedup. They also combine the three modules and show about 2.10x speedup over the original CPU-only implementation.

However, they did not present exactly how they implement their CUDA programs for the three functions nor how they accelerate their programs in [Ahmed et al., 2012].

Device memory access pattern

As described in Section 2.3.1.3, the CUDA memory hierarchy includes registers, local, shared, global, constant and texture memory, as shown in Figure 2.10. Memory throughput generally dominates program performance both in the CPU and GPU domains. Here is a review of how these studies applied different device memory access pattern to optimize their implementations.

[Walters et al., 2009] found the most effective optimization for the Viterbi algorithm is to optimize CUDA memory layout and usage patterns within the implementation. Since the Viterbi algorithm requires only the current and the previous rows of the dynamic programming matrices, they reduce the memory requirements of the Viterbi scoring calculation from $(3 \times M \times L + 5 \times L)$ to $(6 \times M)$ integer array elements, where M and L are the length of the sequence and HMM, respectively.

They note that coalesced access of global memory can significantly improve hmmsearch overall speedup. Their benchmark results show that this single approach contributes an improvement of more than 9x for larger HMMs.

They utilize high speed texture memory to store the target sequences, because the sequence data are static and read-only during computation. They also use texture memory and constant memory to store the query profile HMM depending on its size. They place the normal size HMM in constant memory. In cases where the very large HMM exceeds the capacity of constant memory, they switch over to texture memory for the remaining portion of the HMM after allocating all the constant memory. They utilize shared memory to temporarily store the index into each thread's sequence.

[Du et al., 2010] reorganizes the computational kernel of the Viterbi algorithm, and divides it into two parts: the independent and dependent parts. All of the independent parts are executed in parallel and balances load to optimize the coalesced access to global memory. This significantly improves the performance of the Viterbi algorithm on the GPU.

They implement the *wave-front* pattern using a data skewing strategy. This places cells in the same group to be adjacent to each other. In this way, the data accessed by neighbor threads are adjacent to each other. Therefore threads can access memory in a more efficient manner.

[Quirem et al., 2011] implements the Viterbi algorithm for the Tesla C1060 GPU.

They utilize pinned memory to reduce the latency introduced by transfer memory between device and host. They test two different versions of the memory allocation mechanism: one is pageable memory allocation with the standard *malloc* function, another is pinned memory allocation with the *cudaHostAlloc* function. Pinned memory is host memory that can not be paged (swapped) out to disk by the virtual memory management of the OS, and thus reduces the latency introduced by transfer memory. Based on their experiments, utilizing pinned memory, the kernel execution on the GPU is relatively greater than the transfer time. Kernel execution time is basically the same for both pageable and pinned memory, because the two versions only relate to the speed of the memory transfer. In their experiments, the impact of pinned memory on total computation time is an improvement of roughly 20% over that of non-pinned memory.

Their implementation gains 10x-15x speedup over the original implementation of the Viterbi function according to the number of queries. They tested up to 16,384 queries as that was a limitations of the Tesla C1060 and the speedup increased exponentially as the number of launched threads i.e. number of queries doubled.

Chapter 3

A CUDA accelerated HMMER3 protein sequence search tool

3.1 Requirements and design decisions

The following are the requirements for a CUDA accelerated HMMER3 protein sequence search tool:

- A HMMER3 protein sequence search tool, named *cudaHmmsearch*, will be implemented to run on CUDA-enabled GPU and several optimization will be taken to accelerate the computation. The cudaHmmsearch will be tested and compared with other CPU and GPU implementations.

- The cudaHmmsearch will be based on the HMMER3 algorithm so that the result will be the same as hmmsearch of HMMER3.

- The cudaHmmsearch will be completely usable under various GPU devices and sequence database sizes. This means that cudaHmmsearch is not just for research purpose or just a proof of concept.

Implementation toolkit and language

NVIDIA CUDA [NVIDIA, 2014b] was chosen as the toolkit to be used in the implementation phase. Since its introduction in 2006, CUDA has been widely deployed through

thousands of applications and published research papers, and supported by an installed base of over 500 million CUDA-enabled GPUs in notebooks, workstations, compute clusters and supercomputers [NVIDIA, 2014c]. As of writing, CUDA is the most mature and popular GPU programming toolkit.

HMMER3 is implemented in the C programming language. CUDA provides a comprehensive development environment for C and C++ developers. However, some advanced features of CUDA, such as texture, are only supported in C++ template programming. So C++ has to be used, and some compatibility problems when compiling and programming between C and C++ have also to be dealt with accordingly.

Implementation methods

The following two approaches have been explored for parallelizing the protein sequence database search using CUDA. A target sequence in the database is processed as one task.

- **Task-based parallelism** Each task is assigned to exactly one thread, and *blockDim* tasks are performed in parallel by different threads in a thread block.

- **Data-based parallelism** Each task is assigned to one or many thread block(s) and all threads in the thread block(s) cooperate to perform the task in parallel.

Task-based parallelism has some advantages over data-based parallelism. On one hand, it removes the need for inter-thread communications or, even worse, inter-multiprocessor communications. As described before, the thread or processing elements of one CUDA multiprocessor can communicate by using shared memory, while slow global memory must be used to transfer data between multiprocessors. At the same time, data-based parallelism also needs to take time on synchronizing and cooperating among threads. On the other hand, task-based parallelism is processing one sequence on each thread which results in a kernel where each processing element is doing the exact same thing independently. This also simplifies implementation and testing. Although task-based parallelism needs more device memory than data-based parallelism, it can achieve better performance [Liu et al., 2009]. Thus, the approach of task-based parallelism is taken and efforts are focused on optimizing CUDA kernel execution.

Since data-based parallelism occupies significantly less device memory, [Liu et al., 2009] uses it to support the longest query/subject sequences. However, a different strategy here is applied to work around this problem and is discussed in detail in subsection 3.3.8 on workload distribution.

3.2 A straightforward implementation

This section describes a straightforward, mostly un-optimized implementation of the protein database search tool. First, a simple serial CPU implementation of hmmsearch is presented, with no GPU specific traits. Next, the MSV filter is ported to the GPU. This implementation is then optimized in the next section.

3.2.1 CPU serial version of hmmsearch

The CPU serial version of hmmsearch in HMMER3 is shown in Figure 3.1. The MSV and Viterbi algorithms described in subsection 2.2.2.2 and 2.2.2.3 are implemented in the so-called "acceleration pipeline" at the core of the HMMER3 software package [Eddy, 2011]. One call to the acceleration pipeline is executed for the comparison of each query model and target sequence.

After each filter step, the pipeline either accepts or rejects the entire comparison, based on the P-value of the score calculated in each filter. For example, as can be seen in Figure 3.1, by default a target sequence can pass the MSV filter if its comparison gets a P-value of less than 0.02. In practice about 2% of the top-scoring target sequences are expected to pass the filter. So, much fewer target sequences can pass one filter and hence need further computing. In consequence, the comparison is accelerated. Thus, the first MSV filter is typically the run time bottleneck for hmmsearch. Therefore, the key to parallelizing hmmsearch tool is to offload the MSV filter function to multiple computing elements on the GPU, while ensuring that the code shown in Figure 3 is as efficient as possible.
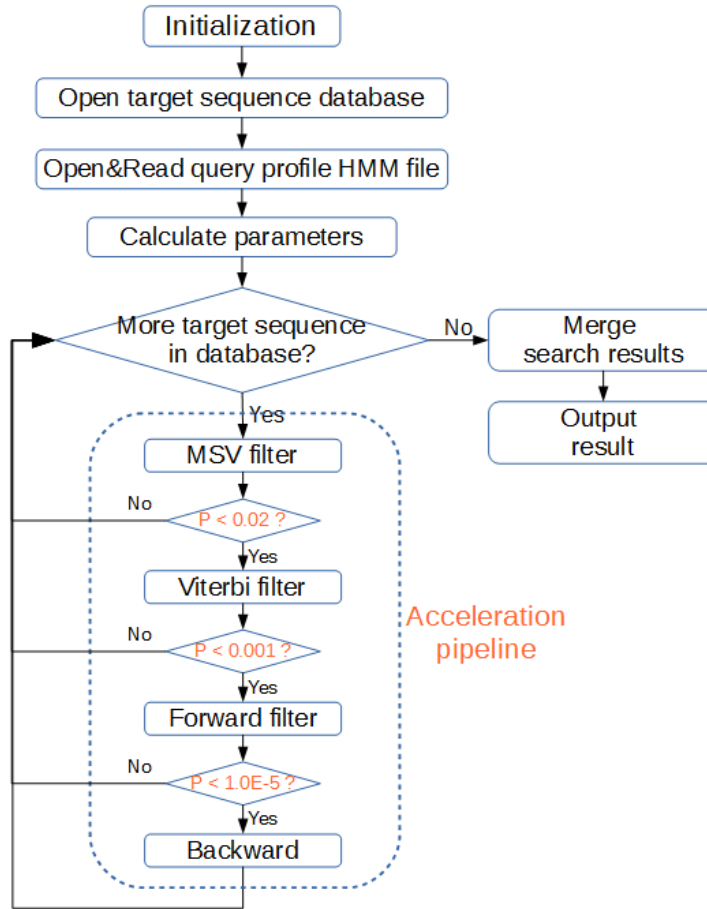
FIGURE 3.1: The CPU serial version of hmmsearch

3.2.2 GPU implementation of MSV filter

A basic flow of the GPU implementation for the MSV filter is shown in Figure 3.2. The code is split up into two parts, with the left *host* part running on the CPU and the right *device* part running on the GPU. There is some redundancy as data needed by the GPU will be copied between the memories in the host and the device.

The CPU code mainly concerns allocating data structures on the GPU, loading data, copying data to the GPU, launching the GPU kernel and copying back the results for further steps.

The GPU kernel code corresponds to the MSV filter Algorithm 3. First, the thread's current database sequence is set to the thread id. Hence each thread begins processing a different neighbouring sequence. This thread id is a unique numeric identifier for each thread and the id numbers of threads in a warp are consecutive. Next, the location where each thread can store and compute its dp matrix is determined in the global
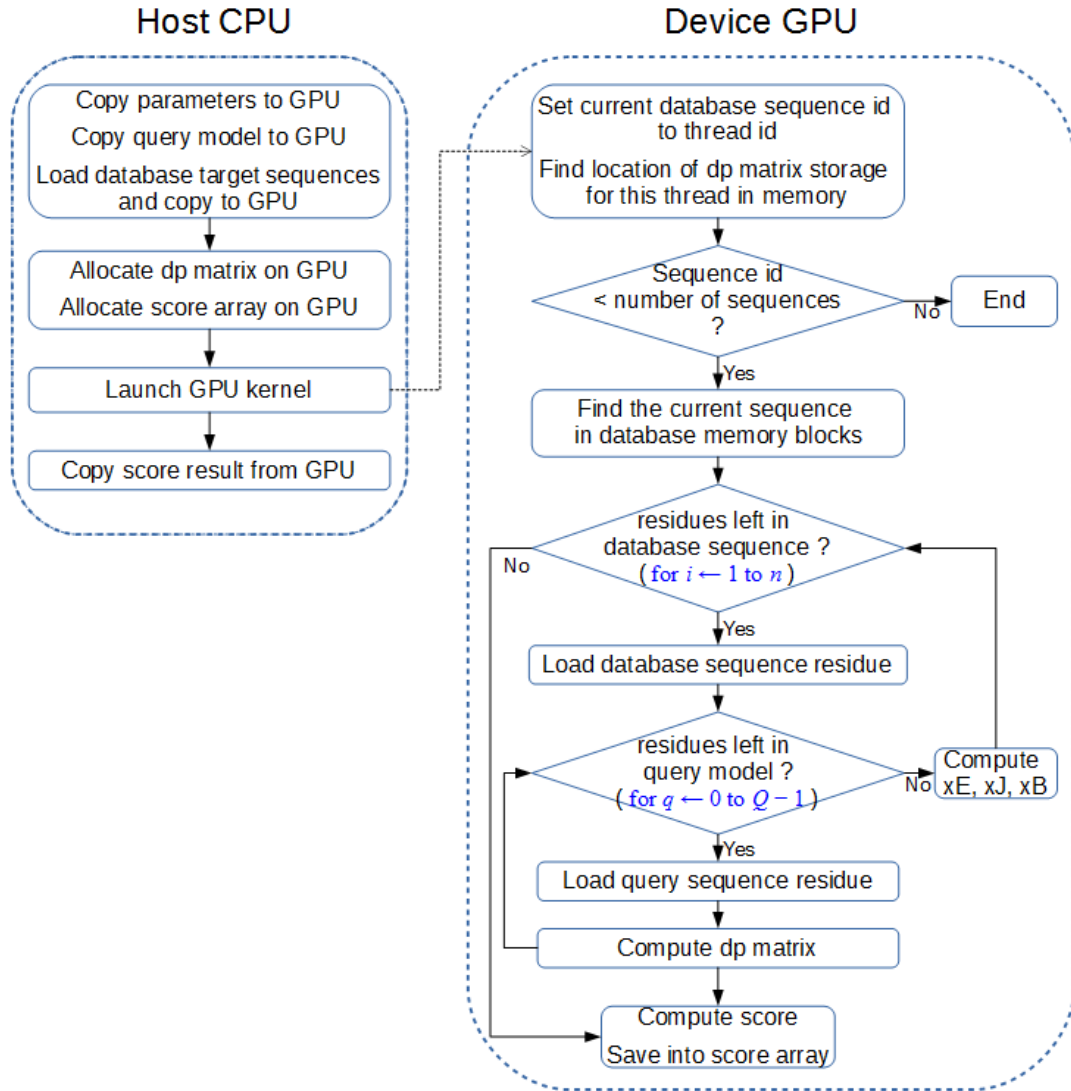
FIGURE 3.2: The GPU porting of MSV filter

memory. This is calculated also using the thread id for each thread. When processing the sequence, successive threads access the successive addresses in the global memory for the sequence data and dp matrix, i.e. using a coalesced access pattern. Execution on the GPU kernel is halted when every thread finishes its sequence.

3.3 Optimizing the implementation

Although a fully functioning GPU MSV filter has been presented, its simple implementation is quite slow: more than 227 seconds to search the test database Swiss-Prot with 540,958 query sequences, as shown in Table 4.2.

This section discusses the optimization steps taken to eventually reach a benchmark database search time of 1.65 seconds: an almost 137 times speedup.

3.3.1 Global Memory Accesses

The global memory is used to store most of data on the GPU. A primary concern in the optimization is to improve the efficiency of accessing global memory. One way is to reduce the frequency of access. Another way is coalescing access.

Access frequency

The elements of the *dp* matrix and the query profile matrix are 8-bit values. The *uint4* and *ulong2* (see the code below) are 128-bit CUDA built-in vector types. So the access frequency would be decreased 16 times by using *uint4* or *ulong2* to fetch the 8-bit values residing in global memory, compared with using 8-bit *char* type.

```
struct __device_builtin__ uint4
{
unsigned int x, y, z, w;
}
struct __device_builtin__ ulong2
{
unsigned long int x, y;
};
```

This approach is very effective and gained a huge speed boost of almost 8 times in total.

Coalescing access

Coalescing access is the single most important performance consideration in programming for CUDA-enabled GPU architectures. Coalescing is a technique applied to combine several small and non-contiguous access of global memory, into a single large and more efficient contiguous memory access. A prerequisite for coalescing is that the words

accessed by all threads in a warp must lie in the same segment. As can be seen in Figure 3.3, the memory spaces referred to by the same variable names (not referring to the same addresses) for all threads in a warp have to be allocated in the form of an array to keep them contiguous in address space.
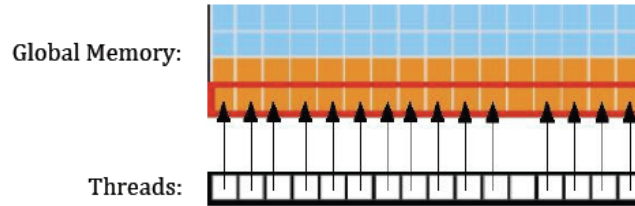
FIGURE 3.3: **Coalescing Global Memory Accesses(Waters, 2011)**. A prerequisite for coalescing access global memory: the addresses of global memory being accessed by the threads in a warp must be contiguous and increasing (i.e., offset by the thread ID).

For coalescing access, the target sequences are arranged in a matrix like an upside-down bookcase shown in Figure 3.4, where all residues of a sequence are restricted to be stored in the same column from top to bottom. And all sequences are arranged in decreasing length order from left to right in the array, which is explained in Section 3.3.7.
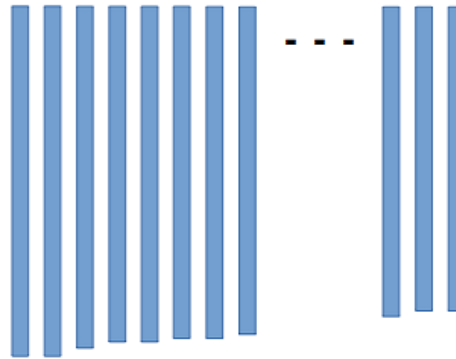
FIGURE 3.4: **Alignment of target sequences** For coalescing access, all residues of a target sequence are stored in the same column of the data matrix from top to bottom. Each thread is in charge of processing a sequence in a column.

Figure 3.5 presents the similar global memory allocation pattern of dp matrix for M processing target sequences. Each thread processes independent dp array with the same length Q. A memory slot is allocated to a thread and is indexed top-to-bottom, and the access to dp arrays is coalesced by using the same index for all threads in a warp.

An alignment requirement is needed to fulfill for fully coalescing, which means any access to data residing in global memory is compiled to a single global memory instruction.
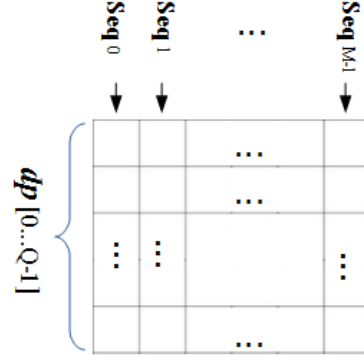
FIGURE 3.5: **The allocation pattern of dp matrix in global memory**. Each thread is in charge of processing a sequence in a column. The sequences are indexed from $Seq0$ to Seq_{M-1}. M is the number of target sequences. The dp matrix has Q rows which corresponds to the profile length.

The alignment requirement is automatically fulfilled for the built-in types like *uint4* [NVIDIA, 2013-05].

The move to vertical alignment of *dp* matrix resulted in an improvement of about 44%.

Note on coding global memory coalescing access

At the beginning, since *uint4* is 16-bytes data block, the traditional C/C++ memory block copy function *memcpy()* was used to copy data between global memory and register memory, as shown in the following code. The *dp* is the pointer to the address of global memory. The *mpv* and *sv* are *uint4* data type residing in register memory.

```
memcpy(&mpv, dp, sizeof(uint4));
memcpy(dp, &sv, sizeof(uint4));
```

However, in practice during CUDA kernel execution, the above *memcpy* involves $16 = sizeof(uint4)$ reads/writes from/to global memory respectively, not one read/write. Switching to the following direct assignment instruction will be one read/write and fully coalesce access global memory, with 81% improvement over the above *memcpy()*.

```
mpv = *(dp);
*(dp) = sv;
```

3.3.2 Texture memory

The read-only texture memory space is a cached window into global memory that offers much lower latency and does not require coalescing for best performance. Therefore, a texture fetch costs one device memory read only on a cache miss; otherwise, it just costs one read from the texture cache. The texture cache is optimized for 2D spatial locality, so threads of the same warp that read texture addresses that are close together will achieve best performance [NVIDIA, 2013-05].

Texture memory is well suited to random access. CUDA has optimized the operation fetching 4 values (RGB colors and alpha component, a typical graphics usage) at a time in texture memory. This mechanism is applied to fetch 4 read-only values from the query profile matrix *texOMrbv* with the *uint4* built-in type. Since the data of target sequences is read-only, it can also use texture memory for better performance.

Switching to texture memory for the query profile texOMrbv resulted in about 22% performance improvement.

Restrictions using texture memory

Texture memory is designed for the GPU graphics processing and therefore is less flexible than the CUDA standard types. It must be declared at compile time as a fixed type, for example *uint4* for the query profile in our case:

texture<uint4, cudaTextureType2D, cudaReadModeElementType> *texOMrbv*;

How the values are interpreted is specified at run time. Texture memory is read-only to the CUDA kernel and must be explicitly accessed via a special texture API (e.g. tex2D(), tex1Dfetch(), etc) and arrays must be bound to textures.

uint4 rsc4 = tex2D(texOMrbv, x, y);

However, on the CUDA next-generation architecture Kepler, the texture cache gets a special compute path, removing the complexity associated with programming it [NVIDIA, 2013-07b].

3.3.3 SIMD Video Instructions

Like Intel SSE2 described in subsection 2.2.2.4, CUDA also provides the scalar SIMD (Single Instruction, Multiple Data) video instructions. These are available on devices of compute capability 3.0. The SIMD video instructions enable efficient operations on pairs of 16-bit values and quads of 8-bit values needed for video processing.

The SIMD video instructions can be included in CUDA programs by way of the assembler, *asm*(), statement.

The basic syntax of an *asm*() statement is:

asm("template-string" : "constraint"(output) : "constraint"(input));

The following three instructions are used in the implementation. Every instruction operates on quads of 8-bit signed values. The source operands ("op1" and "op2") and destination operand ("rv") are all unsigned 32-bit registers ("u32"), which is different from 128-bit CPU registers in SSE2. For additions and subtractions, saturation instructions ("sat") have been used to clamp the values to their appropriate unsigned ranges.

```
/* rv[z] = op1[z] + op2[z] (z = 0,1,2,3) */
asm("vadd4.u32.u32.u32.sat %0, %1, %2, %3;" : "=r"(rv) : "r"(op1), "r"(op2), "r"(0));
/* rv = op1 + op2 */
asm("vsub4.u32.u32.u32.sat %0, %1, %2, %3;" : "=r"(rv) : "r"(op1), "r"(op2), "r"(0));
/* rv = max(op1,op2) */
asm("vmax4.u32.u32.u32 %0, %1, %2, %3;" : "=r"(rv) : "r"(op1), "r"(op2), "r"(0));
```

Switching to the SIMD video instructions also achieved a large speedup of nearly 2 times.

These results, as well as the acceleration of HMMER3, show that the parallel vector instructions can greatly improve computing for array or matrix operations. We can also see the limitation of GPU SIMD computing compared to CPU SIMD computing: the GPU can only support 32-bit register operations, which are 4 times less in data bandwidth than that CPU SSE2 128-bit register operations.

3.3.4 Virtualized SIMD vector programming model

Vector programming model plays an important role in operations of array or matrix. On one hand, it can reduce significantly the frequency of memory access. On the other hand, it can utilize the SIMD vector instructions for parallel computing on the CPU or the GPU.

Inspired by the fact that CUDA has optimized the operation fetching a four component RGBA colour in texture memory, the target sequence is re-organized using a packed data format, where four consecutive residues of each sequence are packed together and represented using the *uchar4* vector data type, instead of the *char* scalar data type, as can be seen in Figure 3.6(*a*). In this way, four residues are loaded using only one texture fetch, thus significantly improving texture memory throughput.
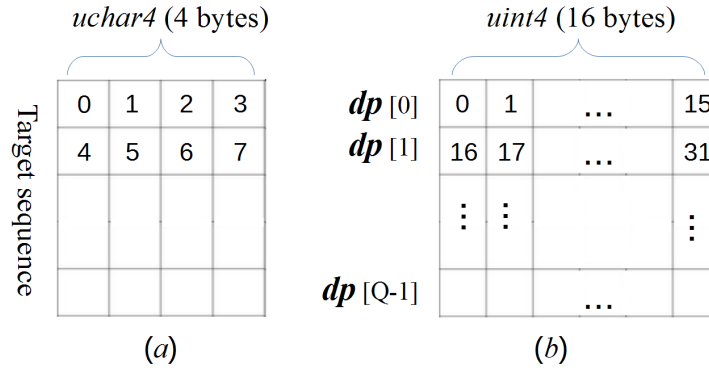
FIGURE 3.6: **SIMD vector alignment pattern**: (*a*) For a target sequence, four consecutive residues which are indexed from 0 are packed together and represented using the uchar4 vector data type. (*b*) For a dp array, 16 consecutive bytes which are indexed from 0 are packed together and represented using the uint4 vector data type. A dp array has Q elements which corresponds to the profile length.

Similarly, the dp array and the query profile also use the virtualized SIMD vector allocation pattern, as can be seen in Figure 3.6(*b*). The reason why the target sequence only use 4-byte uchar4, not 16-byte uint4 as the dp array is because it will demand much more register memory. And the dp array has been packed in this pattern in HMMER3.

3.3.5 Pinned (non-pageable) Memory

It is necessary to transfer data to the GPU over the PCI-E data bus. Compared to the access to CPU host memory, this bus is very slow. Pinned memory is memory that cannot be paged (swapped) out to disk by the virtual memory management of the OS.

In fact, PCI-E transfer can only be done using pinned memory, and if the application does not allocate pinned memory, the CUDA driver does this in the background for us. Unfortunately, this results in a needless copy operation from the regular (paged) memory to or from pinned memory. We can of course eliminate this by allocating pinned memory ourselves.

In the application, we simply replace *malloc/free* when allocating/freeing memory in the host application with *cudaHostAlloc/cudaFreeHost*.

cudaHostAlloc (void** host_pointer, size_t size, unsigned int flags)

3.3.6   Asynchronous memory copy and Streams

Asynchronous memory copy

By default, any memory copy involving host memory is synchronous: the function does not return until after the operation has been completed. This is because the hardware cannot directly access host memory unless it has been page-locked or pinned and mapped for the GPU. An asynchronous memory copy for pageable memory could be implemented by spawning another CPU thread, but so far, CUDA has chosen to avoid that additional complexity.

Even when operating on pinned memory, such as memory allocated with *cudaMallocHost*(), synchronous memory copy must wait until the operation is finished because the application may rely on that behavior. When pinned memory is specified to a synchronous memory copy routine, the driver does take advantage by having the hardware use DMA, which is generally faster [Wilt, 2013].

When possible, synchronous memory copy should be avoided for performance reasons. Keeping all operations asynchronous improves performance by enabling the CPU and GPU to run concurrently. Asynchronous memory copy functions have the suffix *Async*(). For example, the CUDA runtime function for asynchronous host to device memory copy is *cudaMemcpyAsync*().

Asynchronous memory copy works well only where either the input or output of the GPU workload is small and the total transfer time is less than the kernel execution

time. By this means we have the opportunity to hide the input transfer time and only suffer the output transfer time.

Multiple streams

A CUDA stream represents a queue of GPU operations that get executed in a specific order. We can add operations such as kernel launches, memory copies, and event starts and stops into a stream. The order in which operations are added to the stream specifies the order in which they will be executed. CUDA streams enable CPU/GPU and memory copy/kernel processing concurrency. For GPUs that have one or more copy engines, host to/from device memory copy can be performed while the SMs are processing kernels. Within a given stream, operations are performed in sequential order, but operations in different streams may be performed in parallel [Sanders, 2011].

To take advantage of CPU/GPU concurrency as depicted in Figure 3.7, when performing memory copies as well as kernel launches, asynchronous memory copy must be used. Mapped pinned memory can be used to overlap PCI Express transfers and kernel processing.
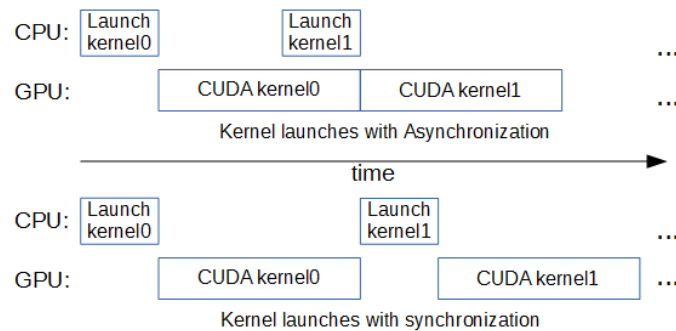
FIGURE 3.7: CPU/GPU concurrency (Wilt, 2013).

CUDA compute capabilities above 2.0 are capable of concurrently running multiple kernels, provided they are launched in different streams and have block sizes that are small enough so a single kernel will not fill the whole GPU.

By using multiple streams, we broke the kernel computation into chunks and overlap the memory copies with kernel execution. The new improved implementation might have the execution timeline as shown in Figure 3.8 in which empty boxes represent time when one stream is waiting to execute an operation that it cannot overlap with the other stream's operation.
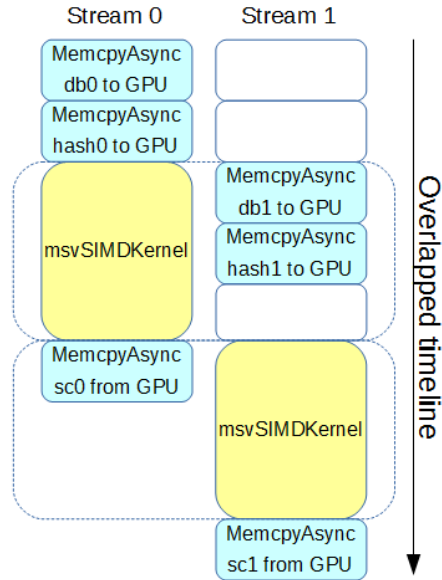
FIGURE 3.8: Timeline of intended application execution using two independent streams.

Running the improved program using pinned memory, asynchronous memory copy and two streams reveals the time drops from 16.45s to just 9.46s; a quite significant drop of over 73.8% in execution time.

3.3.7 Sorting the database

As described in Section 2.2.2.3, the MSV filter function is sensitive to the length of a target sequence, which determines the execution times of the main *for* loop in Algorithm 3.

The target sequence database could contain many sequences with different lengths. The NCBI NR database used in this thesis consists of over 38 million sequences with sequence lengths varying from 6 to 41,943 amino acids [NCBI, 2014].

This brings a problem for parallel processing of threads on the GPU: one thread could be processing a sequence of several thousands of residues while another might be working on a sequence of just a few. As a result, the thread that finishes first might be idle while the long sequence is being handled. Furthermore, unless care is taken when assigning sequences to threads, this effect might be compounded by the heavily unbalanced workload among threads.

In order to achieve high efficiency for task-based parallelism, the run time of all threads in a thread block should be roughly identical. Therefore the database is converted with sequences being sorted by length. Thus, for two adjacent threads in a thread warp, the difference value between the lengths of the associated sequences is minimized, thereby balancing a similar workload over threads in a warp.

Block reading

Many research implementations were not concerned with practical matters. They simply loaded the whole database data into the memories of the CPU host and the GPU device. A large database, like NCBI NR database, is more than 24GB in size, being too large to load into memory of most machines.

Given that the GPU global memory is much less than the CPU host, we use the size of the GPU global memory as the basis to decide the size of the sequence block while reading the database.

Descending order

The memory pools for database sequences both in the CPU host and the GPU device are dynamically allocated at run time. The pools may be required to be reallocated due to more space needed for the current data block than the last one. If the pool allocated at the first time is the largest one during execution, then the overhead of reallocation will be saved. Hence, the descending order is used for sorting the database.

Performance improved

The CUDA profiling tool nvprof [NVIDIA, 2014d] was used to understand and optimize the performance of the MSV GPU application cudaHmmsearch. The nvprof command was used as follows:

```
# nvprof ./cudaHmmsearch globins4.hmm uniprot_sprot.fasta
```

We used the above command twice for profiling cudaHmmsearch execution before and after the target database was sorted. Table 3.1 and 3.2 list the profiling results respectively. The experiments were done in the environment described in Section 4.1. The globins4.hmm is the Globin4 profile HMM and uniprot_sprot.fasta is the SP201309 database, which are also described in Section 4.1.

Time(%)	Time	Calls	Avg	Min	Max	Name
91.61%	4.27108s	134	31.874ms	5.9307ms	137.67ms	msvSIMDKernel
8.37%	390.01ms	271	1.4391ms	704ns	23.027ms	[CUDA memcpy HtoD]
0.01%	556.21us	134	4.1500us	1.7280us	5.9840us	[CUDA memcpy DtoH]
0.01%	491.23us	134	3.6650us	3.4880us	4.0640us	[CUDA memset]

TABLE 3.1: **Profiling result of before sorting database.** Each row is the statistics of profiling result for the function named in the '**Name**'. The statistics includes the percentage of running time, the running time, the number of called times, as well as the average, minimum, and maximum time.

Time(%)	Time	Calls	Avg	Min	Max	Name
97.41%	2.07263s	134	15.467ms	29.056us	194.91ms	msvSIMDKernel
2.54%	54.115ms	271	199.69us	704ns	23.013ms	[CUDA memcpy HtoD]
0.03%	550.53us	134	4.1080us	1.6640us	4.6720us	[CUDA memcpy DtoH]
0.02%	474.90us	134	3.5440us	672ns	4.0320us	[CUDA memset]

TABLE 3.2: **Profiling result of after sorting database.** The meaning of each column is the same as Table 3.1

From the result of profiling, we can see the performance has been increased, which is clearly shown in two ways:

1. the ratio of the msvSIMDKernel run-time to the total increased from 91.61% to 97.41%;

2. the msvSIMDKernel run-time decreased from 4.27108s to 2.07263s and the time of the memory copy from Host to Device (CUDA memcpy HtoD) decreased from 390.01ms to 54.115ms.

This approach has the advantage of being both effective and quite straightforward as a large 129% performance improvement can be gained over the unsorted database without

changing the GPU kernel in any way (see Table 4.2 and Figure 4.1). For the 24GB NCBI NR database used in these experiments, only 6 minutes were taken for sorting. Further, the sorted database can still be usable for other applications, making the one-time cost of sorting it negligible.

3.3.8   Distributing workload

After launching the GPU kernel, the CPU must wait for the GPU to finish before copying back the result. This is accomplished by calling *cudaStreamSynchronize(stream)*. We can get further improvement by distribute some work from the GPU to the CPU while the CPU is waiting. In a protein database, the sequences with the longest or the shortest length are very few. According to Swiss-Prot database statistics [UniProtSP, 2014-05], the percentage of sequences with length > 2500 is only 0.2%. Considering the length distribution of database sequences and based on the descending sorted database discussed in Section 3.3.7, we assigned the first part of data with longer lengths to the CPU. By this way, we can save both the GPU global memory allocated for sequences and the overheads of memory transfer.

The compute power of the CPU and the GPU should be taken into consideration in order to balance the workload distribution between them. The distribution policy calculates a ratio R of the number of database sequences assigned to the CPU, which is calculated as

$$R = \frac{f_C}{N_G f_G + f_C}$$

where f_G and f_C are the core frequencies of the GPU and the CPU respectively, N_G is the number of GPU multiprocessors.

3.3.9   Miscellaneous consideration

This sections discusses various small-scale optimization and explains some techniques not suited to the MSV implementation.

Data type for register memory

In order to reduce the register pressure in the CUDA kernel, we may consider using unsigned 8-bit char type (u8) instead of 32-bit int type (u32). Declaring the registers as u8 results in sections of code to shift and mask data. The extract data macros are deliberately written to mask off the bits that are not used, so this is entirely unnecessary. In fact, around four times the amount of code will be generated if using an u8 type instead of an u32 type.

Changing the u8 definition to an u32 definition benefits from eliminating huge numbers of instructions. It seems potentially to waste some register space. In practice, CUDA implements u8 registers as u32 registers, so this does not actually cost anything extra in terms of register space [Cook, 2013].

Branch divergence

A warp executes one common instruction at a time, so full efficiency is realized when all 32 threads of a warp agree on their execution path. If threads of a warp diverge via a data-dependent conditional branch, the warp serially executes each branch path taken, disabling threads that are not on that path, and when all paths complete, the threads converge back to the same execution path. Branch divergence occurs only within a warp; different warps execute independently regardless of whether they are executing common or disjoint code paths. So the divergence results in some slowdown.

Since the implementation has changed u8 type in register memory to u32 type, the test for the overflow condition is not needed any more. This not only saves several instructions, but also avoids the issue of branch divergence.

Constant memory

Constant memory is as fast as reading from a register as long as all threads in a warp read the same 4-byte address. Constant memory does not support, or benefit from, coalescing, as this involves threads reading from different addresses. Thus, parameters used by all threads, such as $base$, t_{jb}, t_{ec}, are stored into constant memory.

Shared memory

In terms of speed, shared memory is perhaps 10x slower than register accesses but 10x faster than accesses to global memory. However, some disadvantages apply to shared memory.

- Unlike the L1 cache, the shared memory has a per-block visibility, which would mean having to duplicate the data for every resident block on the SM.

- Data must be loaded from global to shared memory in GPU kernel and can not be uploaded to shared memory directly from the host memory.

- Shared memory is well suited to exchange data between CUDA threads within a block. As described in subsection 3.1, task-based parallelism is applied without the need for inter-thread communications, which also saves the cost of synchronization $_{--}syncthreads()$ among threads.

Because of these disadvantages, the MSV implementation does not use shared memory.

Kernel launch configuration

Since the MSV implementation does not use shared memory (as explained above), the following dynamic kernel launch configuration is used to prefer the larger L1 cache and smaller shared memory so as to further improve memory throughput.

```
cudaFuncSetCacheConfig(msvSIMDKernel, cudaFuncCachePreferL1);
```

3.4 Conclusion of optimization

This section briefly reviews the all the optimization approaches discussed in this chapter thus far, and summarizes the steps to gain better performance for CUDA programming.

Six steps to better performance

1. Assessing the application

   In order to benefit from any modern processor architecture, including GPUs, the first step is to assess the application to identify the hotspots [MSV filter in Section 3.2.1], and to identify which type of parallelism [Task-based parallelism in Section 3.1] is better suited to the application.

2. Profiling the application

   NVIDIA provides profiling tools to help identify hotspots and compile a list of candidates for parallelization or optimization on CUDA-enabled GPUs [nvprof in Section 3.3.7], as detailed in Section 2.3.1.4. Intel provides VTune Amplifier XE to collect a rich set of data to tune CPU and GPU compute performance at https://software.intel.com/en-us/intel-vtune-amplifier-xe.

3. Optimizing memory usage

   Optimizing memory usage starts with minimizing data transfers both in size [Database sorted in Section 3.3.7, workload distribution in Section 3.3.8] and time [Pinned Memory in Section 3.3.5] between the host and the device [Asynchronous memory copy in Section 3.3.6]. Be careful with the CUDA memory hierarchy: register memory [Section 3.3.9], local memory, shared memory [Section 3.3.9], global memory, constant memory [Section 3.3.9] and texture memory [Section 3.3.2], and combine these memories to best suit the application [Kernel launch configuration in Section 3.3.9]. Sometimes, the best optimization might even be to avoid any data transfer in the first place by simply recomputing the data whenever it is needed.

   The next step in optimizing memory usage is to organize memory accesses according to the optimal memory access patterns. This optimization is especially important for coalescing global memory accesses [Section 3.3.1].

4. Optimizing instruction usage

   This principle suggests using SIMD Video Instructions [Section 3.3.3] and trading precision for speed when it does not affect the end result, such as using intrinsic instead of regular functions or single precision instead of double precision [HMMER3 in Section 2.2.2.4]. Particular attention should be paid to the control flow instructions [Branch divergence in Section 3.3.9].

5. Maximizing parallel execution

   The application should maximize parallel execution at a higher level by explicitly exposing concurrent execution on the device through streams [Section 3.3.6], as well as maximizing concurrent execution between the CPU host [Database sorted in Section 3.3.7] and the GPU device [Workload distribution in Section 3.3.8 and SIMD Video Instructions in Section 3.3.3].

6. Considering the existing libraries

   Many existing GPU-optimized libraries [NVIDIA, 2014e] such as cuBLAS [NVIDIA, 2014f], MAGMA [MAGMA, 2014], ArrayFire [ArrayFire, 2014], or Thrust [NVIDIA, 2014g], are available to make the expression of parallel code as simple as possible.

Chapter 4

Benchmark results and discussion

Chapter 3 described several approaches to optimize the cudaHmmsearch implementation. This chapter presents the performance measurements when experimenting with these approaches on a GPU and on a multi-core CPU.

4.1   Benchmarking environment

The benchmarking environment was set up in the Kronos 840S desktop workstation produced by Ciara Technologies Inc. [CIARA , 2013] The Kronos has the following configuration:

- CPU host : Intel Core i7-3960X with 6 cores, 3.3GHz clock speed, 64GB RAM

- GPU device : NVIDIA Quadro K4000 graphics card with 3 GB global memory, 768 Parallel-Processing Cores, 811 MHz GPU Clock rate, CUDA Compute Capability 3.0.

- Software system : The operating system used was Ubuntu 64 bit Linux v12.10; the CUDA toolkit used was version 5.5.

The data used in the experiments consisted of :

- Target sequences database : Two target sequences databases was used in the benchmark experiments: **SP201309** and **N201404**. SP201309 was Swiss-Prot

64

database in fasta format released in September 2013 [UniProt, 2013-09] containing
540,958 sequences with length varying from 2 to 35,213 amino acids, comprising
192,206,270 amino acids in total, more than 258MB in file size. N201404 was
much larger NCBI NR database in fasta format released in April 2014 [NCBI,
2014] containing 38,442,706 sequences with length varying from 6 to 41,943 amino
acids, comprising 13,679,143,700 amino acids in total, more than 24GB in file size.

- Query profile HMMs : We tested 5 profile HMMs of length 149, 255, 414, 708 and
  1111 states respectively, detailed in Table 4.1. The globins4 with a length of 149
  states was distributed with the HMMER source [HMMER, 2014a]. The other 4
  HMMs were taken directly from the Pfam database [Pfam, 2013].

Name	globins4	120_Rick_ant	2HCT	ACC_central	AAA_27
Accession number	-	PF12574.3	PF03390.10	PF08326.7	PF13514.1
Length	149	255	414	708	1111

TABLE 4.1: Profile HMMs used in benchmarking. The globins4 has no Accession number.

The measurement of performance that was used was GCUPS (Giga Cell Units Per
Second) which was determined as follows:

- Measuring method

$$GCUPS = \frac{L_q * L_t}{T * 1.0e09}$$

where L_q is the length of query profile HMM, i.e. the number of the HMM states,
L_t is the total residues of target sequences in the database, T is the execution time
in second.

The execution time of the application was timed using the C clock() instruction.
All programs were compiled using GNU g++ with the -O3 option and executed
independently in a 100% idle system.

4.2 Performance Results

We did four experiments for our implementation cudaHmmsearch benchmarking. Each experiment was done in the same benchmarking environment as described in Section 4.1. This section will explain each experiment and show the results and the related analysis of these experiments.

4.2.1 Comparison with less optimized approaches

Experiment A : This experiment tested the performance of cudaHmmsearch with several selected approaches. To show the performance impact of the selected optimization approaches, the performance of the corresponding implementation was benchmarked and the corresponding improvement was measured in percentage compared with that of previous approach. All tests were taken searching the globins4 profile HMM against the SP201309 database.

Description of approach	Execution time (s)	Performance (GCUPS)	Improvement (%)
Initial implementation	227.178	0.126	-
SIMD Video Instruction	125.482	0.228	81
Minimizing global memory access	16.449	1.741	664
Async memcpy & Multi streams	9.463	3.026	74
Coalescing of global memory	6.565	4.362	44
Texture memory	5.370	5.333	22
Sorting Database	2.346	12.207	129
Distributing workload	1.650	17.357	42

TABLE 4.2: **Performance of optimization approaches.** The table shows the result of Experiment A, using cudaHmmsearch to search the globins4 profile HMM against the SP201309 database. The fourth column **Improvement** is measured in percentage compared with the previous approach. The row 'Coalescing of global memory' is benchmarked only for the dp matrix. The row 'Texture memory' is benchmarked only for the query profile texOMrbv 2D texture.

Table 4.2 shows the testing results of ExperimentA. The fourth column 'Improvement' is measured in percentage compared with the previous approach. 'Initial implementation' described in Section 3.2 is used as the baseline. 'SIMD Video Instruction' is the approach

described in Section 3.3.3. 'Minimizing global memory access' is the approach of reducing the frequency of global memory access described in Section 3.3.1. 'Async memcpy & Multi streams' is the approach described in Section 3.3.6. 'Coalescing of global memory' is the approach of coalescing access described in Section 3.3.1. 'Texture memory' is the approach described in Section 3.3.2. 'Sorting Database' is the approach described in Section 3.3.7. 'Distributing workload' is the approach described in Section 3.3.8.

The graphic view corresponding to the above table is shown in Figure 4.1.
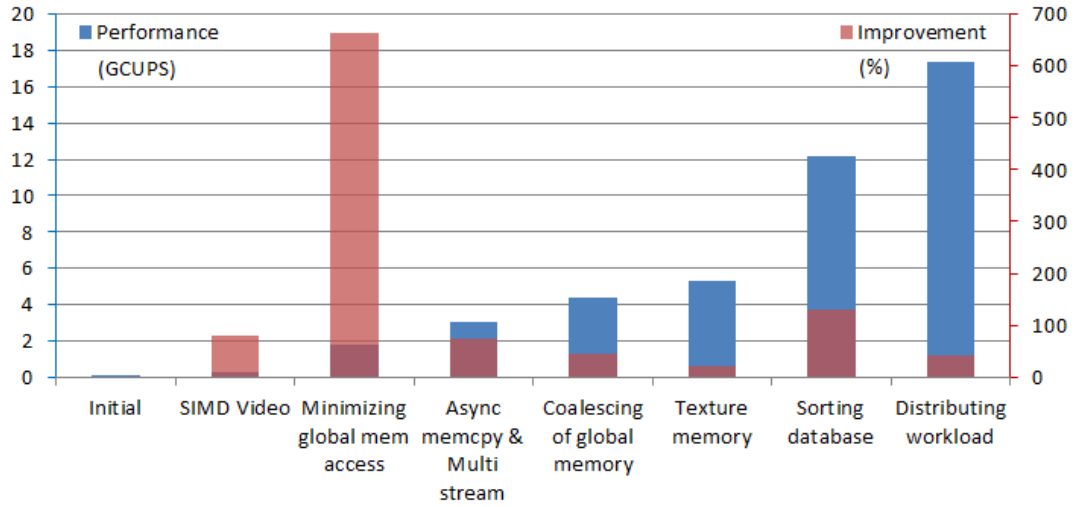
FIGURE 4.1: **Performance of optimization approaches.** The data of this chart come from Table 4.2 for Experiment A. The blue bar is Performance (in GCUPS) of each approach, corresponding to the left Y axis. The red bar is Improvement in % corresponding to the right Y axis.

From Figure 4.1, it can be seen that the global memory optimizations are the most important area for performance. Several factors are related to global memory accesses, including the highest 663% minimizing global memory access, coalescing of global memory and texture memory. To make all threads in a warp execute similar tasks, the auxiliary sorting database also plays an important role in optimizations.

4.2.2 Practical benchmark

Experiment B : This experiment tested the real-world performance of the final cudaHmmsearch implementation, with the optimizations discussed in Chapter 3. This was done by using the fully optimized cudaHmmsearch to search the much large N201404 database for the 5 profile HMMs in Table 4.1. As comparison, the same searches were

executed by hmmsearch of HMMER3 on one CPU core on the Kronos machine. The result of Experiment B is shown in Table 4.3.

Profile HMM (length)	hmmsearch (s) (GCUPS)		cudaHmmsearch (s) (GCUPS)		Speedup (times)
globins4 (149)	217.54s	9.37GCUPS	88.63s	23.00GCUPS	2.45
120_Rick_ant (255)	297.52s	11.72GCUPS	108.42s	32.17GCUPS	2.74
2HCT (414)	484.68s	11.68GCUPS	188.72s	30.01GCUPS	2.57
ACC_central (708)	809.97s	11.96GCUPS	295.02s	32.83GCUPS	2.75
AAA_27 (1111)	2203.36s	6.90GCUPS	1034.96s	14.68GCUPS	2.13
Average	-		-		2.53

TABLE 4.3: **Result of Practical benchmark.** The table shows the result of Experiment B, using the fully optimized cudaHmmsearch and hmmsearch of HMMER3 to search the 5 profile HMMs against the N201404 database. In the column of hmmsearch and cudaHmmsearch, the left sub-column is execution time in second and the right sub-column is performance in GCUPS. Speedup is measured in times of cudaHmmsearch performance over that of hmmsearch.

The results of the benchmarks are shown in graphical form in Figure 4.2. The GPU cudaHmmsearch performance hovers just above 25 GCUPS, while the CPU hmmsearch only around 10 GCUPS. The whole performance of cudaHmmsearch is stable with various lengths of query HMMs. On average, cudaHmmsearch has a speedup of 2.53x over hmmsearch.

Figure 4.2 also shows that the performance of both GPU and CPU searching for AAA_27 dropped significantly compared with other searches. The reason can be seen from Table 4.4 listing the internal pipeline statistics summary for searching globins4 and AAA_27. Table 4.4 shows the total number of target sequences in the N201404 database and the number of passed sequences after each filter. After every filter, the number of passed sequences for searching AAA_27 with 1111 states is much more than that of globins4 with 149 states. This means that for searching AAA_27, more target sequences are processed than globins4 in each filter after the MSV filter. At the same time, each of these filters is more time-consuming than the MSV filter. This results in the AAA_27 performance dropping significantly.
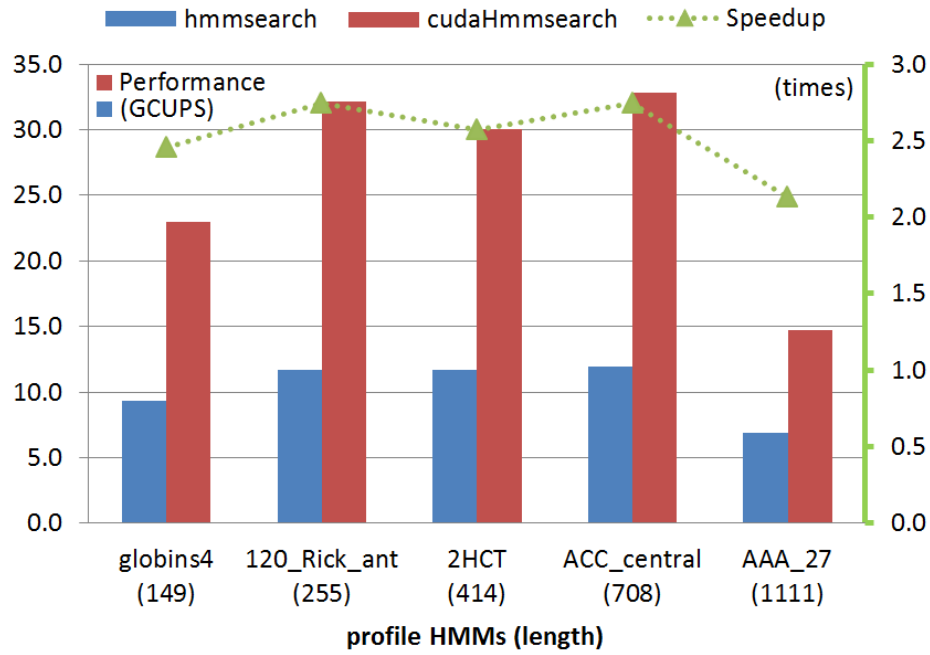
FIGURE 4.2: **Practical benchmarks.** The data of this chart come from Table 4.3. The blue and red bar is Performance (in GCUPS) of hmmsearch and cudaHmmsearch respectively, corresponding to the left Y axis. The green dot line is Speedup (in times) of cudaHmmsearch performance over that of hmmsearch, corresponding to the right Y axis.

Query profile HMM(length)	globins4 (149 states)	AAA_27 (1111 states)
Target sequences	38442706	38442706
Passed MSV filter	1195043	4305846
Passed bias filter	973354	1671084
Passed Viterbi filter	70564	322206
Passed Forward filter	7145	17719

TABLE 4.4: **Internal pipeline statistics summary.** The table shows the total number of target sequences in the N201404 database and the number of passed sequences after each filter for searching globins4 and AAA_27 in the Experiment B.

4.2.3   Comparison with multicore CPU

Experiment C :   This experiment tested the performance of cudaHmmsearch and hmmsearch of HMMER3 running with multiple CPU cores. The Kronos experiment system has an Intel Core i7-3960X CPU with six cores.

A benchmark to study the impact of multiple CPU cores has not been used in the articles cited in this thesis. The purpose of Experiment C is to show how the performance increase or decrease with the use of more CPU cores.

The experiment was done by executing the fully optimized cudaHmmsearch and hmmsearch of HMMER3 with one to six CPU cores, searching the N201404 database for the 120_Rick_ant profile HMM. The result of Experiment C is shown in Table 4.5.

Performance (GCUPS)	1 CPU core	2 CPU cores	3 CPU cores	4 CPU cores	5 CPU cores	6 CPU cores
cudaHmmsearch	32.17	50.22	57.70	59.14	59.39	59.29
hmmsearch	11.72	23.28	29.22	44.15	46.19	44.69
Speedup (times)	2.74	2.16	1.97	1.34	1.29	1.33

TABLE 4.5: **Result of Comparison with multicore CPU.** The table shows the result of Experiment C, using the fully optimized cudaHmmsearch and hmmsearch of HMMER3 to search the 120_Rick_ant profile HMM against the N201404 database with one to six CPU cores involved in computing.

The graphic view of the benchmark is shown in Figure 4.3. The number above each bar is the Performance in GCUPS. As can be seen, from 1 CPU core to 4 CPU cores, both cudaHmmsearch performance and hmmsearch performance increase almost linearly. From then on, perhaps due to complex scheduling among CPU cores and only one I/O to load sequences from the database for CPU cores, the extra CPU cores do not contribute much to either cudaHmmsearch or hmmsearch execution. Even worse, six CPU cores have a negative effect compared to five CPU cores.
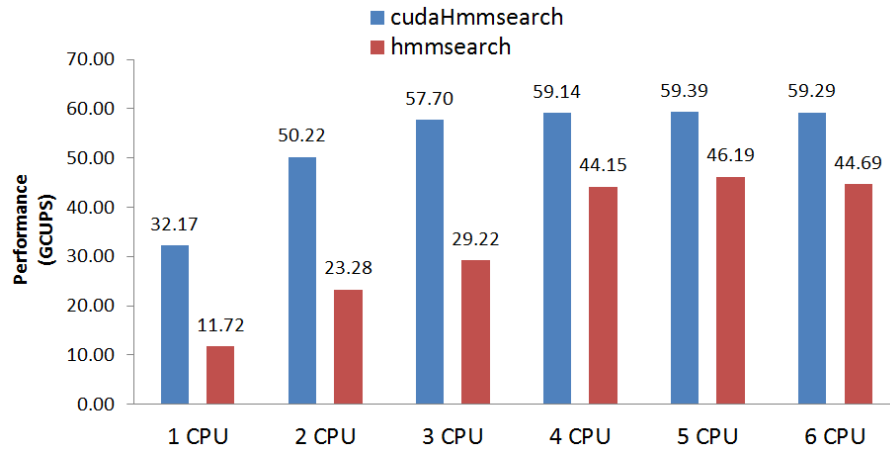

FIGURE 4.3: **Comparison with multicore CPU.** The data of this chart come from Table 4.5 for Experiment C. The number above each bar is the Performance in GCUPS.

4.2.4   Comparison with other implementations

Experiment D :   This experiment tested the performance of cudaHmmsearch with previous hmmsearch solutions: HMMER2.3.2 [HMMER2.3.2, 2003], GPU-HMMER2.3.2 [Walters et al., 2009] and HMMER3 [HMMER, 2014a]. All tests were taken using the fully optimized cudaHmmsearch and the hmmsearch in HMMER2.3.2, GPU-HMMER2.3.2 and HMMER3 to search against the SP201309 database for the globins4 profile HMM. The hmmsearch in HMMER2.3.2 and HMMER3 were executed on one CPU core. The hmmsearch in GPU-HMMER2.3.2 was executed on one GPU using one CPU core. The result of Experiment D is shown in Table 4.6.

Application (Device)	HMMER2.3.2 (CPU)	GPU-HMMER2.3.2 (GPU)	HMMER3 (CPU)	cudaHmmsearch (GPU)
Performance (GCUPS)	0.14	0.95	8.47	17.36
Speedup (times)	1.00	6.79	60.50	124.00

TABLE 4.6: **Result of Comparison with other implementations.** The table shows the result of Experiment D, searching against the SP201309 database for the globins4 profile HMM. The hmmsearch in HMMER2.3.2 and HMMER3 were executed on one CPU core. The hmmsearch in GPU-HMMER2.3.2 and the fully optimized cudaHmmsearch was executed on one GPU using one CPU core. Speedup uses the performance of HMMER2.3.2 as baseline 1.00 and is measured in times of each performance over that of HMMER2.3.2.

As seen from the Figure 4.4, since the release of HMMER2.3.2 in Oct 2003, accelerating hmmsearch researches on both CPU and GPU have achieved significant improvement.
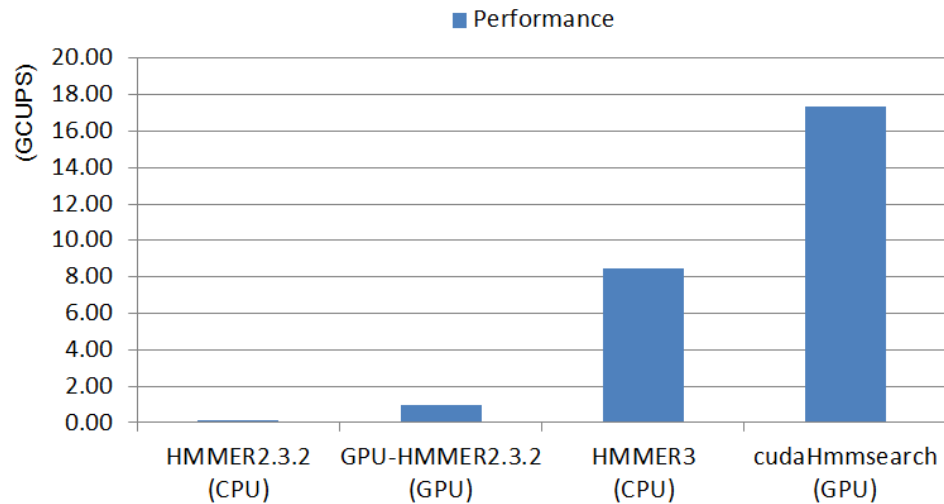

FIGURE 4.4: **Comparison with other implementations**. The data of this chart come from Table 4.6 for Experiment D.

Chapter 5

Conclusions

A fully-featured and accelerated HMMER3 protein search tool *cudaHmmsearch* was implemented on CUDA-enabled GPU. It can search the protein sequence database for profile HMMs.

5.1   Summary of Contributions

Our research work started with dynamic programming, the common characteristic of Swith-Waterman algorithm, Viterbi algorithm and MSV algorithm, which are famous protein sequence alignment algorithms in Bioinformatics. We summarized the technologies of accelerating Swith-Waterman algorithm on a CUDA-enabled GPU, which has been widely researched. We also briefly presented GPU acceleration work related to Viterbi algorithm.

After analyzing the core application *hmmsearch* in HMMER3, we found the key hotspot MSV filter for accelerating hmmsearch. We presented the details of our *cudaHmmsearch* implementation and optimization approaches. At the same time, we also discussed and analyzed the advantages and limitations of GPU hardware for CUDA parallel programming. Then we summarized six steps for better performance of CUDA programming: 1)assessing the application; 2)profiling the application; 3)optimizing memory usage; 4)optimizing instruction usage; 5)maximizing parallel execution; 6)considering the existing libraries.

We performed comprehensive benchmarks. The results were analyzed and the efficiency of the *cudaHmmsearch* implementations on the GPUs was demonstrated. We achieved 2.5x speedup over the single-threaded HMMER3 CPU SSE2 implementation. The performance analysis showed that GPUs are able to deal with intensive computations, but are very sensitive to random accesses to the global memory.

The solutions in this thesis were designed and customized for current GPUs, but we believe that the principles studied here will also apply to future many-core GPU processors, provided the GPU is CUDA-enabled. Here is the complete list of CUDA-enabled GPUs: https://developer.nvidia.com/cuda-gpus.

5.2 Limitations of Work

There are some weak points in our work summarized as follows:

Although our *cudaHmmsearch* can search against an unsorted protein sequence database, it gains 129% improvement by searching against a sorted database according to benchmark Table 4.2. Although the program for sorting database is provided, the user may be unaware of this and run *cudaHmmsearch* against an unsorted database. It is better for the program to evaluate the database automatically and prompt the user to sort if necessary.

We use a block reading method to process very large databases. However, the number of sequences for each block reading is fixed. Hence the number of threads launched in GPU kernel is also fixed. For those sequences with shorter lengths, it is better to use dynamic block reading to load more sequences, so as to increase the occupancy of GPU threads and achieve better performance.

5.3 Recommendations for Future Research

The limitations noted in the last section call attention to several areas that we deem worthy of further improvement and investigation. The suggested topics are placed under the following headings.

Forward filter for no threshold

By default, the top-scoring of target sequences are expected to pass each filter. Alternatively, the --*max* option is available for those who want to make a search more sensitive to get maximum expected accuracy alignment. The option causes all filters except the Forward/Backward algorithm to be bypassed. According to practical benchmarking in Section 4.2.2, the performance decreased greatly due to much more calculation in the Forward algorithm. So our next research should be focused on accelerating the Forward algorithm on a CUDA-enabled GPU.

Multiple GPUs approach

Since currently we have no multiple GPUs within a single workstation, we did not research on multiple GPUs approach. However, CUDA already provides specific facilities for multi-GPU programming, including threading models, peer-to-peer, dynamic parallelism and inter-GPU synchronization, etc. Almost all PCs support at least two PCI-E slots, allowing at least two GPU cards to insert almost any PC. Looking forward, we should also investigate multi-GPU solutions.

Appendix A

Resource of this thesis

The code of *cudaHmmsearch* and this thesis has submitted to Google subversion server powered by Google Project Hosting and can be accessed in a web browser or subversion client with the address: http://cudahmmsearch.googlecode.com/svn/trunk/.

Bibliography

[Ahmed et al., 2012] Fahian Ahmed, Saddam Quirem, Gak Min and Byeong Kil Lee. *Hotspot Analysis Based Partial CUDA Acceleration of HMMER 3.0 on GPGPUs.* International Journal of Soft Computing and Engineering (IJSCE) ISSN: 2231-2307, Volume-2, Issue-4, September 2012.

[Aji et al., 2008] S. Aji, F. Blagojevic, W. Feng, D.S. Nikolopoulos. *Cell-Swat: Modeling and Scheduling Wavefront Computations on the Cell Broadband Engine.* Proceedings of the 2008 ACM International Conference on Computing Frontiers 13-22.

[Akoglu and Striemer, 2009] Ali Akoglu and Gregory M. Striemer. *Scalable and highly parallel implementation of Smith-Waterman on graphics processing unit using CUDA.* Springer Science+Business Media, LLC 2009.

[Altschul et al., 1990] S. F. Altschul, W. Gish, W. Miller, E. W. Myers and D. J. Lipman. *Basic local alignment search tool.* Journal of Molecular Biology, 215(3):403–10, October 1990.

[ArrayFire, 2014] AccelerEyes. Comprehensive GPU function library. Website, 2014. URL http://www.accelereyes.com/.

[CIARA, 2013] CIARA Technologies Inc. KRONOS 840S Desktop Workstation. Website, 2013. URL http://www.ciaratech.com/product.php?id_prod=489&lang=en&id_cat1=1&id_cat2=9&id_cat3=129.

[Cook, 2013] Shane Cook. *CUDA Programming : A Developer's Guide to Parallel Computing with GPUs.* Elsevier Inc. USA, 2013.

[Baldi and Brunak, 2001] Pierre Baldi and Soren Brunak. *Bioinformatics: The Machine Learning Approach.* The MIT Press, England, 2nd edition, 2001.

[Derrien and Quinton, 2007] S. Derrien and P. Quinton. *Parallelizing HMMER for hardware acceleration on FPGAs.* Proceedings of the 18th IEEE International Conference on Application-Specific Systems, Architectures, and Processors; 911 July 2008.

[Dong and Pei, 2007] Guozhu Dong and Jian Pei. *Sequence Data Mining.* Springer Science+Business Media, LLC, New York, USA, 2007.

[Du et al., 2010] Zhihui Du, Zhaoming Yin, and David A. Bader. *A Tile-based Parallel Viterbi Algorithm for Biological Sequence Alignment on GPU with CUDA.* Parallel & Distributed Processing, Workshops and Phd Forum (IPDPSW), 2010 IEEE International Symposium on , vol., no., pp.1,8, 19-23 April 2010.

[Durbin et al., 1998] Richard Durbin, Sean Eddy, Anders Krogh, and Graeme Mitchison. *Biological sequence analysis: Probabilistic models of proteins and nucleic acids.* Cambridge University Press, New York, USA, 1998.

[Eddy, 2011] Sean R. Eddy. *Accelerated profile HMM searches.* PLoS Comput Biol 7(10): e1002195. doi:10.1371/journal.pcbi.1002195, October 2011. URL http://www.ploscompbiol.org.

[Eidhammer et al., 2004] Ingvar Eidhammer, Inge Jonassen, and William R. Taylor. *Protein Bioinformatics: An Algorithmic Approach to Sequence and Structure Analysis.* John Wiley & Sons, New Jersey, USA, 2004.

[Farrar, 2007] Michael Farrar. *Striped Smith-Waterman speeds database searches six times over other SIMD implementations.* Bioinformatics 23: 156-161 2007.

[Ganesan et al., 2010] Narayan Ganesan, Roger D. Chamberlain, Jeremy Buhler, and Michela Taufer. *Accelerating HMMER on GPUs by Implementing Hybrid Data and Task Parallelism.* Proc. of ACM International Conference on Bioinformatics and Computational Biology, August 2010, pp. 418-421.

[Gotoh, 1982] O. Gotoh. *An improved algorithm for matching biological sequences.* J. Mol. Biol 1982, 162:705-708.

[Hancock and Zvelebil, 2004] John M. Hancock and Marketa J. Zvelebil, editors. *Dictionary of Bioinformatics and Computational Biology.* John Wiley & Sons, New Jersey, USA, 2004.

[Henikoff and Henikoff, 1992] S. Henikoff and J.G. Henikoff. *Amino Acid Substitution Matrices from Protein Blocks*. PNAS 89 (22): 10915-10919. doi:10.1073/pnas.89.22.10915. PMC 50453. PMID 1438297, 1992.

[HMMER, 2014a] Howard Hughes Medical Institute. HMMER source code release archives. Website, 2014. URL http://hmmer.janelia.org/software/archive.

[HMMER, 2014b] Howard Hughes Medical Institute. HMMER. Website, 2014. URL http://hmmer.janelia.org/.

[HMMER2.3.2, 2003] Howard Hughes Medical Institute. HMMER2.3.2 source code release. Website, 2003. URL http://selab.janelia.org/software/hmmer/2.3.2/hmmer-2.3.2.tar.gz.

[Horn et al., 2005] Daniel Horn, Mike Houston, and Pt Hanrahan. *ClawHMMER: A Streaming HMMer-Search Implementation*. presented at Supercomputing 2005, Washington, D.C., 2005.

[Intel, 2013] Intel. Intel VTune Amplifier XE 2013. Website, 2013. URL https://software.intel.com/en-us/intel-vtune-amplifier-xe/.

[Jacob et al., 2007] A. Jacob, J. Lancaster, J. Buhler, R.D. Chamberlain. *Preliminary results in accelerating profile HMM search on FPGAs*. Proceedings of the 21st IEEE International Parallel and Distributed Processing Symposium; 2630; California, USA. IPDPS 2007.

[Kentie, 2010] M.A. Kentie. *Biological Sequence Alignment Using Graphics Processing Units*. Master thesis (2010), Delft University of Technology.

[Kirk and Hwu, 2010] David B. Kirk and Wen-mei W. Hwu. *Programming Massively Parallel Processors : A Hands-on Approach*. Published by Elsevier Inc. 2010.

[Krogh et al., 1994] A. Krogh, M. Brown, I. S. Mian, K. Sjolander and D. Haussler. *Hidden Markov models in computational biology: Applications to protein modeling*. J. Mol. Biol., 235:1501-1531. 1994.

[Landman et al., 2006] J. Landman, J. Ray, J.P. Walters. *Accelerating HMMer searches on Opteron processors with minimally invasive recoding*. Proceedings of the 20th International Conference on Advanced Information Networking and Applications; 1820;

Vienna, Austria. AINA 2006. URL http://ieeexplore.ieee.org/stamp/stamp.jsp?tp=&arnumber=1620450.

[Lesk, 2008] Arthur M. Lesk. *Introduction to Bioinformatics*. Oxford University Press, New York, USA, 3rd edition, 2008.

[Ligowski and Rudnicki, 2009] Lukasz Ligowski and Witold Rudnicki. *An Efficient Implementation Of Smith Waterman Algorithm On GPU Using CUDA, For Massively Parallel Scanning Of Sequence Databases*. IEEE 2009.

[Liu et al., 2009] Yongchao Liu, Douglas Maskell and Bertil Schmidt. *CUDASW++: optimizing smith-waterman sequence database searches for cuda-enabled graphics processing units*. BMC Research Notes 2, no. 1, 73. 2009. URL http://www.biomedcentral.com/1756-0500/2/73.

[Liu et al., 2010] Yongchao Liu, Bertil Schmidt, and Douglas Maskell. *cudasw++2.0: enhanced smith-waterman protein database search on cuda-enabled gpus based on simt and virtualized simd abstractions*. BMC Research Notes 2010. URL http://www.biomedcentral.com/1756-0500/3/93.

[Liu et al., 2013] Yongchao Liu, Adrianto Wirawan and Bertil Schmidt. *CUDASW++ 3.0: accelerating Smith-Waterman protein database search by coupling CPU and GPU SIMD instructions*. BMC Bioinformatics 2013. URL http://www.biomedcentral.com/1471-2105/14/117.

[Loewy et al., 1991] Ariel G. Loewy, Philip Siekevitz, John R. Menninger and Jonathan A. N. Gallant. *Cell Structure & Function : An Integrated Approach*. Saunders College Publishing, 3rd edition, 1991.

[Isa et al., 2012] M. Nazrin M. Isa, Khaled Benkrid and Thomas Clayton. *A Novel Efficient FPGA Architecture for HMMER Acceleration*. IEEE, 2012.

[Maddimsetty, 2006] R.P. Maddimsetty. *Acceleration of Profile-HMM Search for Protein Sequences in Reconfigurable Hardware*. [Masters thesis]. Washington University in St.Louis.

[MAGMA, 2014] The University of Tennesse. A collection of next generation linear algebra (LA) GPU accelerated libraries MAGMA. Website, 2014. URL http://icl.cs.utk.edu/magma/software/.

[Manavski, 2008] Svetlin A Manavski and Giorgio Valle. *CUDA compatible GPU cards as efficient hardware accelerators for Smith-Waterman sequence alignment.* BMC Bioinformatics 2008. URL http://www.biomedcentral.com/1471-2105/9/S2/S10.

[Markel and Leon, 2003] Scott Markel and Darry Leon. *Sequence Analysis in a Nutshell.* O'Reilly & Associates, Inc., USA, 2003.

[Microsoft, 2013-11] Microsoft. Compute shader overview. Website, 2013-11. URL http://msdn.microsoft.com/en-us/library/windows/desktop/ff476331%28v=vs.85%29.aspx.

[Microsoft, 2013-12] Microsoft. Programming guide for HLSL. Website, 2013-12. URL http://msdn.microsoft.com/en-us/library/windows/desktop/bb509635%28v=vs.85%29.aspx.

[NCBI, 2014] National Center for Biotechnology Information, U.S. National Library of Medicine. NCBI NR (non-redundant) Protein Database. Website, 2014-4-7. URL ftp://ftp.ncbi.nih.gov/blast/db/FASTA/nr.gz.

[Needleman and Wunsch, 1970] S. B. Needleman and C. D. Wunsch. *A general method applicable to the search for similarities in the amino acid sequence of two proteins.* Journal of Molecular Biology, 48(3):443–53, March 1970.

[NVIDIA, 2013-05] NVIDIA. CUDA C PROGRAMMING GUIDE. Website, PG-02829-001_v5.5 May 2013. URL http://docs.nvidia.com/cuda/cuda-c-programming-guide/index.html.

[NVIDIA, 2013-07a] NVIDIA. CUDA C Best Practices Guide. Website, DG-05603-001_v5.5 July 2013. URL http://docs.nvidia.com/cuda/cuda-c-best-practices-guide/index.html.

[NVIDIA, 2013-07b] NVIDIA. Kepler Tuning Guide. Website, July 19, 2013. URL http://docs.nvidia.com/cuda/kepler-tuning-guide/index.html.

[NVIDIA, 2014a] NVIDIA. Directcompute NVIDIA developer zone. Website, 2014. URL https://developer.nvidia.com/directcompute.

[NVIDIA, 2014b] NVIDIA. NVIDIA CUDA zone. Website, 2014. URL https://developer.nvidia.com/cuda-zone.

[NVIDIA, 2014c] NVIDIA. NVIDIA What is CUDA?. Website, 2014. URL `https://http://www.nvidia.com/object/cuda_home_new.html`.

[NVIDIA, 2014d] NVIDIA. Profiler User's Guide. Website, 2014. URL `http://docs.nvidia.com/cuda/profiler-users-guide/`.

[NVIDIA, 2014e] NVIDIA. GPU-accelerated libraries. Website, 2014. URL `https://developer.nvidia.com/gpu-accelerated-libraries`.

[NVIDIA, 2014f] NVIDIA. CUDA Basic Linear Algebra Subroutines (cuBLAS) library. Website, 2014. URL `https://developer.nvidia.com/cublas`.

[NVIDIA, 2014g] NVIDIA. A powerful library of parallel algorithms and data structures. Website, 2014. URL `https://developer.nvidia.com/thrust`.

[Oliver et al., 2007] T. Oliver, L.Y. Yeow, B. Schmidt. *High performance database searching with HMMer on FPGAs.* Proceedings of the 21st IEEE International Parallel and Distributed Processing Symposium; 2630; California, USA. IPDPS 2007.

[OpenCL, 2014] Khronos Group. The open standard for parallel programming of heterogeneous systems. Website, 2014. URL `https://www.khronos.org/opencl/`.

[PassMark, 2014] PassMark Software. CPU Benchmarks. Website, 2014-06. URL `http://www.cpubenchmark.net/high_end_cpus.html`.

[Pevsner, 2009] Jonathan Pevsner. *Bioinformatics and Functional Genomics.* John Wiley & Sons, New Jersey, USA, 2nd edition, 2009.

[Pfam, 2013] Wellcome Trust Sanger Institute and Howard Hughes Janelia Farm Research Campus. Pfam database. Website, March 2013. URL `ftp://ftp.sanger.ac.uk/pub/databases/Pfam/releases/Pfam27.0/Pfam-A.hmm.gz`.

[Quirem et al., 2011] Saddam Quirem, Fahian Ahmed, and Byeong Kil Lee. *CUDA Acceleration of P7Viterbi Algorithm in HMMER 3.0.* 30th IEEE Internationa Performance Computing and Communications Conference (IPCCC), 2011.

[Rognes and Seeberg, 2000] T. Rognes and E. Seeberg. *Six-fold speed-up of Smith-Waterman sequence database searches using parallel processing on common microprocessors.* Bioinformatics 16: 699-706 2000.

[Rognes, 2011] T. Rognes. *Faster Smith-Waterman database searches with inter-sequence SIMD parallelization.* BMC Bioinformatics 2011, 12:221.

[Sachdeva et al., 2008] Vipin Sachdeva, Michael Kistler, Evan Speight, Tzy-Hwa Kathy Tzeng. *Exploring the viability of the Cell Broadband Engine for bioinformatics applications.* Parallel Computing, High-Performance Computational Biology 34:616626. URL http://www.sciencedirect.com/science/article/pii/S0167819108000501.

[Saeed et al., 2010] Ali Khajeh Saeed, Stephen Poole and J. Blair Perot. *Acceleration of the Smith-Waterman algorithm using single and multiple graphics processors.* Journal of Computational Physics 229 (2010) 4247-4258.

[Sanders, 2011] Jason Sanders and Edward Kandrot. *CUDA by example : an introduction to general-purpose GPU programming.* NVIDIA Corporation 2011.

[Smith and Waterman, 1981] TF. Smith and MS. Waterman. *Identification of common molecular subsequences.* Journal of Molecular Biology 1981, 147:195-197.

[UniProtSP, 2014-05] SIB Bioinformatics Resource Portal. UniProtKB/Swiss-Prot protein knowledgebase release 2014-05 statistics. Website, 2014-05. URL http://web.expasy.org/docs/relnotes/relstat.html.

[UniProtTr, 2014-05] EMBL-EBI, Wellcome Trust Genome Campus. UniProtKB/TrEMBL PROTEIN DATABASE RELEASE 2014_05 STATISTICS. Website, 2014-05. URL http://www.ebi.ac.uk/uniprot/TrEMBLstats.

[UniProt, 2013-09] Universal Protein Resource. UniProt Release. Website, 2013-09. URL ftp://ftp.uniprot.org/pub/databases/uniprot/previous_releases/release-2013_09/.

[UniProt, 2014] Universal Protein Resource. About UniProt. Website, 2014. URL http://www.uniprot.org/help/about.

[Walters et al., 2006] J. P. Walters, B. Qudah, and V. Chaudhary. *Accelerating the HMMER Sequence Analysis Suite Using Conventional Processors.* In AINA'6: Proceedings of the 20th International Conference on Advanced Information Networking and Applications, pages 289-294, Washington, DC, USA, 2006. IEEE Computer Society.

[Walters et al., 2009] J. P. Walters, V. Balu, S. Kompalli, and V. Chaudhary. *Evaluating the use of GPUs in Liver Image Segmentation and HMMER Database Searches.* International Parallel and Distributed Processing Symposium (IPDPS), 2009.

[Waters, 2011] Blue Waters. *Taking CUDA to Ludicrous Speed.* Undergraduate Petascale Education Program, Website, June 2011. URL `http://iclcs.uiuc.edu/index.php/iclcs-news/51-blue-waters-undergraduate-petascale-internship-program.html`.

[Wiki Cell, 2014] Wikipedia. Cell (biology). Website, 2014. URL `http://en.wikipedia.org/wiki/Cell_(biology)`.

[Wiki Sequence, 2014] Wikipedia. Sequence Alignment. Website, 2014. URL `http://en.wikipedia.org/wiki/Sequence_alignment`.

[Wilt, 2013] Nicholas Wilt. *The CUDA Handbook : A Comprehensive Guide to GPU Programming.* Pearson Education, Inc. 2013.

[Wun et al., 2005] B. Wun, J. Buhler, and P. Crowley. *Exploiting coarsegrained parallelism to accelerate protein motif finding with a network processor.* In PACT '05: Proceedings of the 2005 International Conference on Parallel Architectures and Compilation Techniques, 2005.

[Zeller, 2008] Cyril Zeller. *Tutorial CUDA.* NVIDIA Developer Technology, 2008.